

NANoREG

Grant Agreement Number 310584

Deliverable D 2.7

Characteristics of test aerosols using different generation methods for inhalation studies

Due date of deliverable: 2016/08/31

Actual submission date: 2016/09/15

Author(s) and company:	Sébastien Bau(INRS), Olivier Witschger (INRS), Ismo Koponen (NRCWE), Keld Jensen (NRCWE), François Gaie Levrel (LNE), Anders Gudmundsson (LTH), Jenny Rissler (LTH)
Work package/task:	WP2 / Tasks 2.4.d and 2.4.h
Document status:	final
Confidentiality:	public
Key words:	aerosol, characterization

DOCUMENT HISTORY

Version	Date	Reason of change
1	2016/08/31	1 st draft
2	2016/09/15	2 nd draft
3	2016/12/09	Final version
4	2017/03/26	Final version following MC comments
5	2017/04/18	Project Office harmonized lay-out

This work is licensed under the Creative Commons Attribution-NonCommercial-ShareAlike 4.0 International License.

To view a copy of this license, visit <http://creativecommons.org/licenses/by-nc-sa/4.0/> or send a letter to Creative Commons, PO Box 1866, Mountain View, CA 94042, USA.

*This project has received funding from the European Union
Seventh Framework Programme (FP7/2007-2013)
under grant agreement no 310584*



Lead beneficiary for this deliverable: Institut National de Recherche et de Sécurité, INRS, partner 21

Owner(s) of this document	
Owner of the content	INRS, Partner 21
Co-Owner 1	NRCWE, Partner 4
Co-Owner 2	LTH, Partner 37
Co-Owner 3	LNE, Partner 47

Table of Content

1	DESCRIPTION OF TASK	4
2	DESCRIPTION OF WORK & MAIN ACHIEVEMENTS	4
2.1	SUMMARY	4
2.2	BACKGROUND OF THE TASK	5
2.3	DESCRIPTION OF THE WORK CARRIED OUT	6
3	LITERATURE REVIEW	6
4	APPLICATION OF AEROSOL CHARACTERIZATION STRATEGY TO DIFFERENT GENERATION METHODS FOR INHALATION STUDIES	10
4.1	INTRODUCTION	10
4.2	CHARACTERISTICS OF AEROSOLS FROM DIFFERENT GENERATION/DISPERSION SYSTEMS	10
4.2.1	Dry-based method – Vibrating air velocity jet generator (NANEUM PA-100S)	10
4.2.1.1	Description of the experimental setup	10
4.2.1.2	Experimental results	12
4.2.1.3	Conclusions	14
4.2.2	Dry-based method – Rotating Brush Generator (PALAS RBG1000)	15
4.2.2.1	Description of the experimental setup	15
4.2.2.2	Case of titanium dioxide nanomaterials	16
4.2.2.3	Case of silica nanomaterials	25
4.2.2.4	Case of other oxide nanomaterials	30
4.2.2.5	Repeatability of aerosol generation according to the mass concentrations	36
4.2.2.6	Conclusions	37
4.2.3	Direct-synthesis method – Spark discharge generator (SDG) and evaporation/condensation in a high temperature (HT) furnace.	40
4.2.3.1	Description of the experimental set-up	40
4.2.3.2	Results obtained for Au, Cu, Pd and Ag aerosols	40
4.2.3.3	Exposure estimation (particle number, surface area, and mass size distribution)	43
4.2.3.4	Comparison of different on-line aerosol instruments for airborne nanoparticles.	44
4.2.3.5	Conclusion	44
4.3	CHARACTERISTICS OF AEROSOLS PRODUCED IN A SYSTEM FOR INHALATION STUDIES	46
4.3.1	NANOTIREX (Nanomaterial Toxicology Inhalation system for Rodent Exposure, INRS)	46
4.3.1.1	Case of titanium dioxide produced by the rotating brush generator (PALAS RBG1000)	47
4.3.1.2	Case of carbon nanotubes produced by a dry acoustic generator	51
4.3.2	NRCWE	56
4.3.2.1	Chemicals	56
4.3.2.2	Generation of test atmospheres and aerosol characterization	56
4.4	EVALUATION AND CONCLUSIONS	59
5	DEVIATIONS FROM THE WORK PLAN	60
6	REFERENCES	60

1 Description of task

The objective of this task was to review and test methods to generate and characterize test aerosols for inhalation studies for in vivo studies. Of this work, recommendations should be made in terms of characterization and monitoring of test aerosols for inhalation studies.

2 Description of work & main achievements

2.1 Summary

In experimental toxicology, when simulating human exposure to aerosols in the working environment, inhalation is the route of administration of choice for evaluating the toxicity of a given material (in aerosol form) in animals. On the subject of the risks related to nanomaterials, the question of the optimal strategy to be taken into account for the test aerosols administered to animals in the case of inhalation studies has been raised for several years. However, this issue is not fully resolved to date.

In this context, this work aimed to contribute to the establishment of recommendations concerning the characterization of aerosol tests in inhalation toxicology studies. Thus, it aims to provide some answers to the proposed refined set of key questions from a regulatory perspective to be addressed in NANoREG, in particular questions on the measurement and characterization (N°1), and on metrology and dose metrics (N°4).

To achieve this aim, the work consisted of 1) reviewing the scientific literature so as to make recommendations not in terms of methods for producing test aerosols but rather to characterize these test aerosols; 2) characterizing, through experimental work, test aerosols using different generation methods to be used for inhalation toxicology studies.

The first part was conducted mainly by LNE and INRS, while the second was conducted by the four partners INRS, LNE, LTH and NRCWE.

An extensive overview of the literature regarding aerosol measurement and characterization for toxicological purpose was performed. In this review, the measurement devices (time integrated/resolved, size integrated/resolved, etc.) as well as the main results were gathered. From the literature review, recommendations for characterizing and monitoring test aerosols for inhalation toxicology studies are proposed. To the extent that relevant and quality data are required, this measurement strategy requires a high level of expertise in aerosol measurement, and the monitoring during the entire duration of the exposure phase of animals. Both parts involve time-resolved size-resolved instruments as well as sampling for subsequent physicochemical characterization.

In the second part of the project, an important experimental work was carried out to test several aerosol generation methods (dry-based method, direct-synthesis method). With the dry-based method, several of the core nanomaterials have been investigated (TiO₂, SiO₂, ZnO, CeO and BaSO₄).

The applied dry-based methods cover the particle size range from about a few tens of nanometers up to several micrometers, the particles and are mainly composed of aggregates and/or agglomerates. The conditions required for inhalation studies (stability, repeatability, level of concentration) are sometimes difficult to obtain, but possible. It is necessary to carry out preliminary tests to ascertain the performances of the chosen devices and their suitability for the inhalation facility, and specialized expertise is needed for in-depths characterization. The applied direct-synthesis methods cover particle size range from about a few nanometers up to several hundred of nanometers. With these methods, higher concentrations in number can be obtained. Stability and repeatability is in general very good.

The work carried out shows that generation and characterization of test aerosols for inhalation toxicology studies is a complex but essential element of inhalation studies. The application of the developed measurement strategy during the NANoREG project has proven to be feasible.

2.2 Background of the task

The inhalation toxicity of nanomaterials is of particular concern in ensuring the health of workers and consumers.

Among the in vivo studies, and although it has the disadvantage of a high demand in costs, the inhalation is still the highly preferred route of exposure as prescribed in OECD Test Guidelines, and therefore considered as a “gold” standard as it is based on “realistic” exposure scenario. Indeed, the major advantage of inhalation exposure is that it mimics human pulmonary exposure by distributing the inhaled material throughout the whole respiratory tract in a physiological way over time (Oberdörster et al, 2015).

Two different approaches are considered in an experimental inhalation study:

- Risk-oriented (agglomerates > 100nm)
- Hazard-oriented (primary nano-objects and small agglomerates < 100nm)

An essential element is that nanomaterials to be dispersed and suspended in air to perform inhalation experiments. To achieve this, various methods have so far been employed; they can be categorized into the three methods shown schematically in Figure 1: wet-based, dry-based or direct synthesis (Morimoto et al., 2012).

In that context, various methods have so far been developed and employed to generate NM and HARN tests aerosols for inhalation studies (Motzkus et al., 2014).

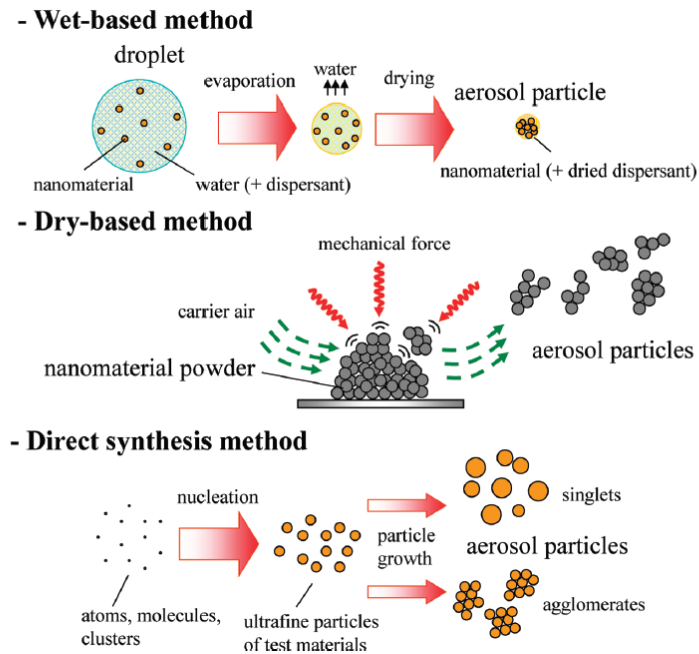


Figure 1: Schematic illustration of methods for generating test aerosols of nanomaterials. Wet-based method, dry-based method, and direct synthesis method are representative ones in inhalation systems (Morimoto et al., 2012).

2.3 Description of the work carried out

As a first step, a literature review has been performed by LNE (Partner 47). From this 75-page report, recommendations for characterizing and monitoring test aerosols through inhalation studies are made (Figure 3).

As a second step, experimental works have been performed by four partners (4, 21, 37 and 47) in order to characterize different test aerosols using different generation methods to be used for inhalation studies. During this second step, some of the experiments have been conducted onto inhalation facilities.

3 Literature review

The inhalation toxicity of nanomaterials is of particular concern in ensuring the health of workers and consumers. Among the in vivo studies, and although it has the disadvantage of a high demand in costs, the inhalation is still the highly preferred route of exposure as prescribed in OECD Test Guidelines, and therefore considered as a “gold” standard as it is based on “realistic” exposure scenario.

The report of the WPMN Expert Meeting of Inhalation Toxicity Testing for Nanomaterials (OECD, 2012a) mentions the need for careful aerosol generation and characterization, and gives examples of reference techniques for generation of exposure atmospheres (Figure 2).

Dispersion technique	Vehicle	Characterisation of exposure atmosphere	Devices
Risk-oriented approach (agglomerates; >100nm)			
Dry dispersion with pressurised air	Clean air	Aerosol concentration (particle mass; particle number); MMAD	Jet mill, venturi, rotating brush generator, Wright Dust feeder, ceramic electrical heater
Nebulisation of a liquid formulation	e.g. phosphate buffer	Aerosol concentration (particle mass; particle number); MMAD; nanoparticle-specific chemical analysis of filter samples for determination of dose	Jet nebuliser
+CNT: acoustic feeder system (subacute, sub chronic testing)	Clean air	Aerosol concentration (particle mass); MMAD: to be calculated based on filter samples/SEM	Membrane system to bring the individual/respirable agglomerates of CNT into the airborne state
CNT: Nebulisation of a liquid formulation (acute testing)	DPPC, BSA, Glucose solution	Aerosol concentration (particle mass); MMAD: to be calculated based on filter samples/SEM	Ultrasonic finger facilitating proper dispersion; no vortexing
Hazard-oriented approach (small agglomerates; < 100nm)			
Spark generation (abrasion of a metal electrode)	Argon, clean air	Aerosol concentration (particle number); mean mobility diameter	Electrical mobility spectrometer

Figure 2: Example of few methods used to generate test aerosols for inhalation studies according to the two approaches (risk- or hazard-orientated) (OECD, 2012b).

An extensive overview of the literature regarding aerosol measurement and characterization for toxicological purpose was performed by LNE (Motzkus et al., 2014). In this review, the measurement devices (time integrated/resolved, size integrated/resolved, etc.) as well as the main results were gathered.

The issues of strategies and data analysis (dose) are also of interest for inhalation exposure systems. Two different levels can be distinguished:

- the aerosol monitoring involves basic measurements allowing the major characteristics of the aerosol to be followed/monitored (e.g. mass or number concentration);
- the aerosol characterization requires a certain expertise to use specific instruments; the latter devices allow the aerosols to be in-depth characterized (e.g. morphology, state of charge, size distribution).

From the literature review performed in this project, recommendations are proposed that are illustrated on Figure 3. These recommendations relate to both the characterization of the aerosol that requires a high level of expertise in aerosol measurement, and the monitoring during the entire duration of the exposure phase of animals. Both parts involve time-resolved size-resolved instruments as well as sampling for subsequent physico-chemical characterization.

As mentioned in section 4.3.1, a typical application of this diagram relies on the use of: (1) a CPC 3007 for the on-line measurement of total submicron particle concentration, (2) an OPC (e.g. PALAS, Fidas Mobile) for the monitoring of airborne particle number size distribution, and (3) systematic Closed-Face Cassette (CFC) samples taken twice a day at a different sampling point to describe aerosol average mass concentration. It is important to note that preliminary data obtained with a CPC 3007 placed at different

points of the facility are obtained to check aerosol homogeneity. These two steps can be carried out by toxicologists, once trained.

Aerosol in-depth characterization involves the participation of aerosol metrologists since it relies on the use of complex measurement techniques, whose results often require more expertise to be interpreted. For instance, time-resolved instruments such as Scanning Mobility Particle Sizer (SMPS), Aerodynamic Particle Sizer (APS) or Electrical Low Pressure Impactor (ELPI) can be used to determine airborne particle number size distribution. Each of the abovementioned instruments has a different size range. Thus, the use of different techniques in parallel can be relevant when the whole size range from few nm to tens of μm is sought. It is also reminded that each technique measures airborne particles according to one of their physical property (equivalent diameter); this can lead to a better physical description of these particles when multiple instruments are used in parallel. Time-integrated sampling for subsequent analysis (TEM, chemical composition) is also of great importance to best characterize the aerosols produced. Last, the use of cascade impactors associated with gravimetric analysis of the impaction stages is the only technique available to describe the mass size distribution of the aerosols. Again, such strategy is illustrated by the example of the NANOTIREX facility in section 4.3.1 (see also Cosnier et al., 2016).

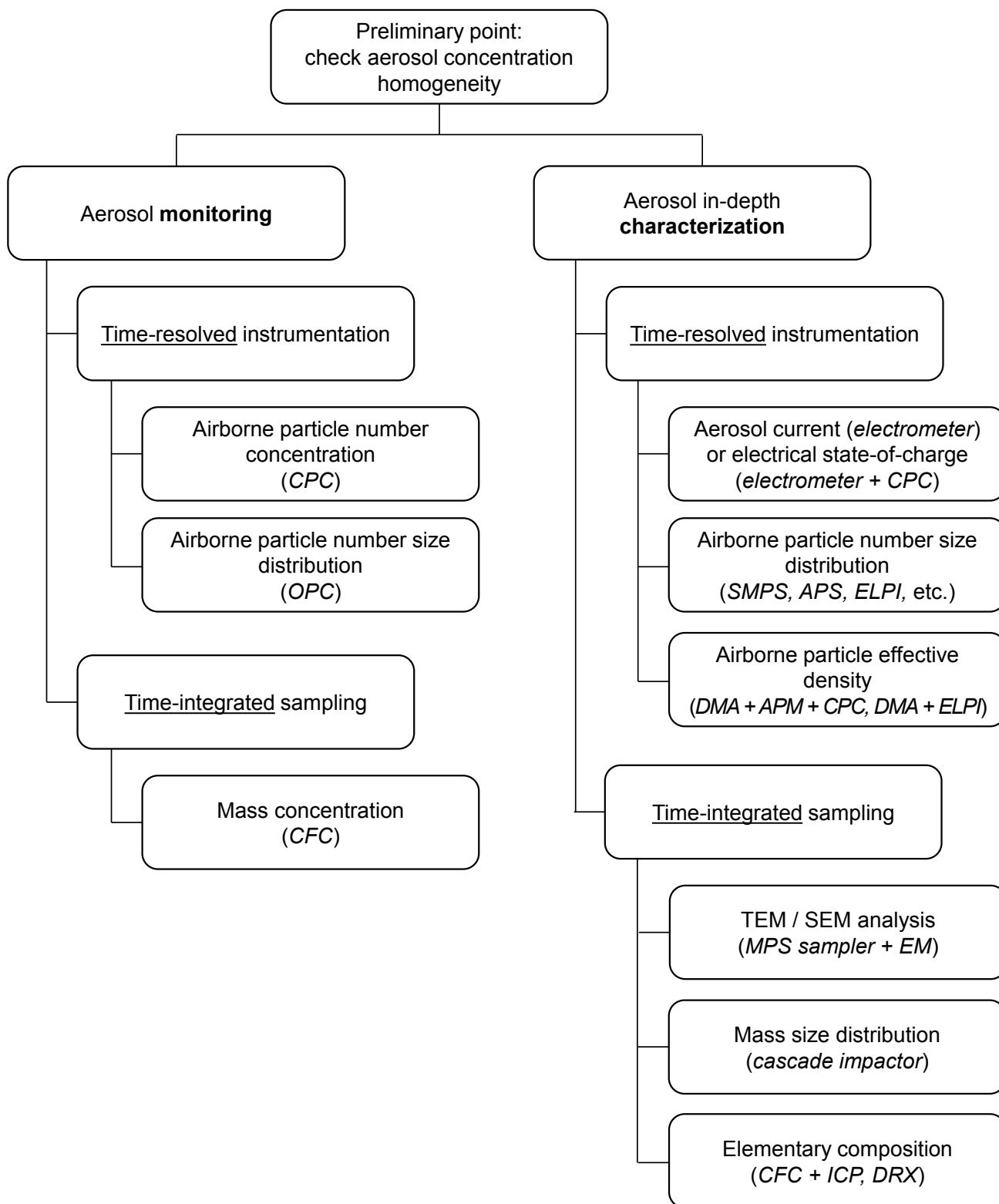


Figure 3: Recommendations for characterizing and monitoring test aerosols for inhalation studies.

4 Application of aerosol characterization strategy to different generation methods for inhalation studies

4.1 Introduction

As stated earlier, there is a need for harmonizing methods of aerosol characterization for different approaches considered in inhalation studies. On that basis, it is hoped that it would enable better comparability in inhalation toxicology results.

4.2 Characteristics of aerosols from different generation/dispersion systems

4.2.1 Dry-based method – Vibrating air velocity jet generator (NANEUM PA-100S)

LNE with INRS implemented jointly an experimental set-up composed of a vibrating air velocity jet generator (NANEUM PA100S). The aerosols were measured simultaneously with a Scanning Mobility Particler Sizer (SMPS) and an Aerodynamic Particle Sizer (APS). This generation system was investigated with only one nanomaterial (NM105).

The main aim of this experimental work was to describe the performances of this generator to produce stable and reproduceable aerosols. Thus, the objectives were (1) to find out two conditions of generations to produce (a) airborne primary particles or small aggregates/agglomerates with the smallest size 100 nm – 300 nm from nanopowders, and (b) airborne agglomerated/aggregated particles with a size close to 1 µm; (2) to evaluate the stability of the number concentration and the size distribution over the time on a continuous generation time of 3 hours.

4.2.1.1 Description of the experimental setup

The PA100S Powder Aerosoliser is based on the vortex shaker principle. This method allows to generate aerosol from powder by concentrating high velocity vibrating jets of clean air at the powder surface, disturbing and separating particles from the powder to create an aerosol. Vortices are formed by the opposing air flows inside the aerosolisation chamber which act to further break apart the aerosol particles. A mechanical agitation system sited at the base of the aerosolisation chamber disturbs the bulk powder and assists the air jets in the generation of aerosol.

The PA100S consists of a pressure regulator feeding the main aerosol flow meter which sets the outlet flow of the instrument. A second bypass flow meter limits the flow through the aerosoliser chamber, and provides aerosol dilution. The two flows are recombined in a high volume gravitational separator (11 liters) where larger particles of the measured aerosol are removed on the basis of gravitational settling. The gravitational separator is also used to stabilise the aerosol concentration. Aerosol concentration can be controlled by adjusting the pressure supplied to the chamber, the flow meter settings and the position of the jet nozzle in relation to the surface of the aerosolising powder. The concentration of the aerosol generated depends strongly on the proximity of the jet nozzle to the powder surface, which is adjustable.

A schematic of the experimental setup is provided in Figure 4.

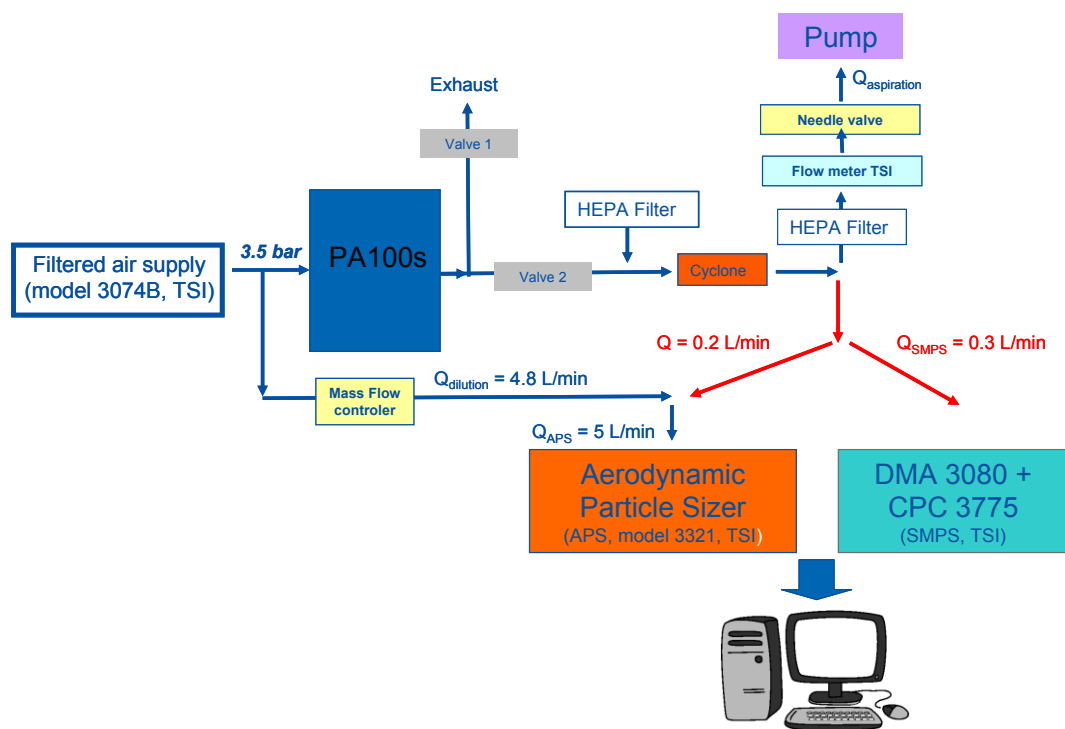


Figure 4: Experimental set-up used for aerosolization of nanostructured powder with the PA100S Powder Aerosoliser

The experimental conditions of generations for PA100s are given in Table 1.

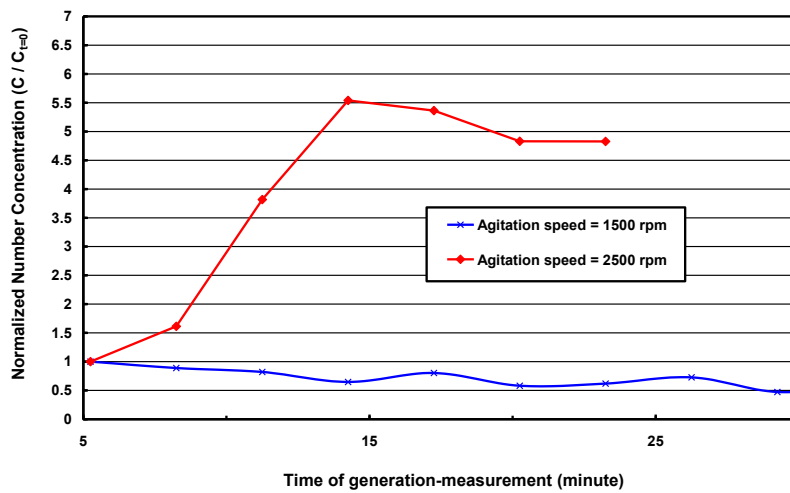
Table 1: Experimental conditions of generations for PA100s: configuration 1.

Regulator pressure indicator gauge	Aerosol outlet flow meter	By pass flow meter	Nozzle travel speed	Agitation speed	Distance between the surface powder and the Nozzle	volume of powder used
1.2 bar	10 L/min	8 L/min; 7 L/min ; 6.5 L/min ; 6 L/min	30 mm/h	1500 rpm and 2500 rpm	10 cm	10 cm ³

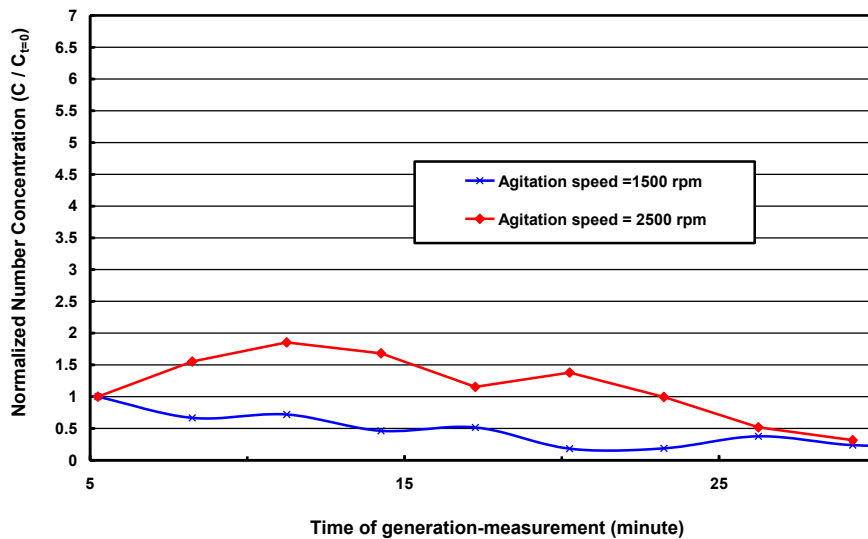
4.2.1.2 Experimental results

First experiments showed a very high concentration of the larger particles measured by APS at the beginning of the generation, which were above the APS upper concentration limit ($> 10^3$ particles/cm³). Thus, the APS was implemented a dilution line by a factor of 25, as drawn in Figure 4, to decrease airborne particle concentration.

Figure 5 present the evolution of the normalized number concentration of airborne particles measured by SMPS (a) and by APS (b) with a bypass flow rate of 8 L/min with the different agitation speeds (1500 and 2500 rpm). The results for SMPS measurement presented were obtained with only the diffusion corrections.



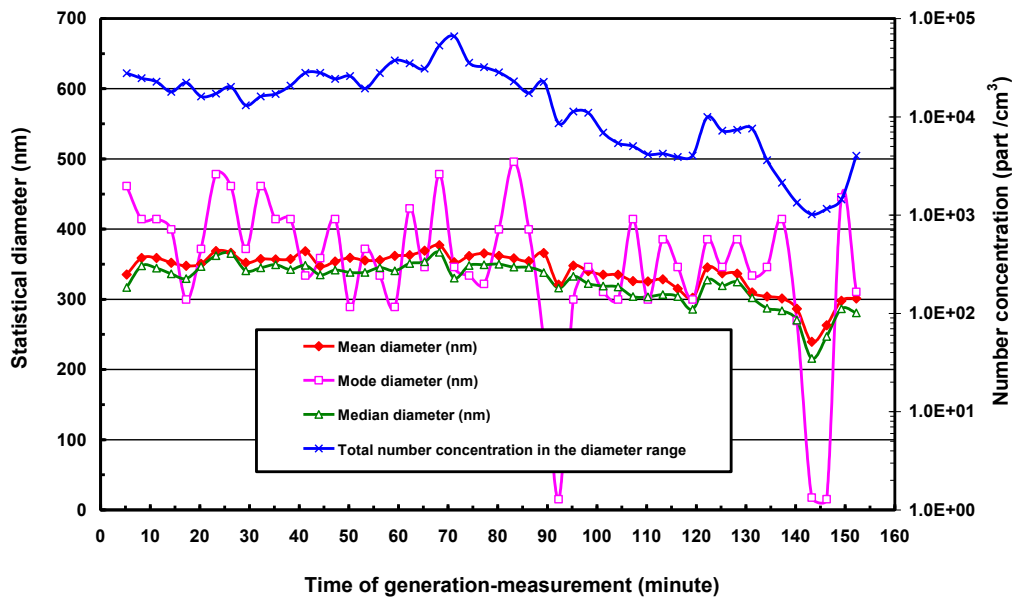
a)



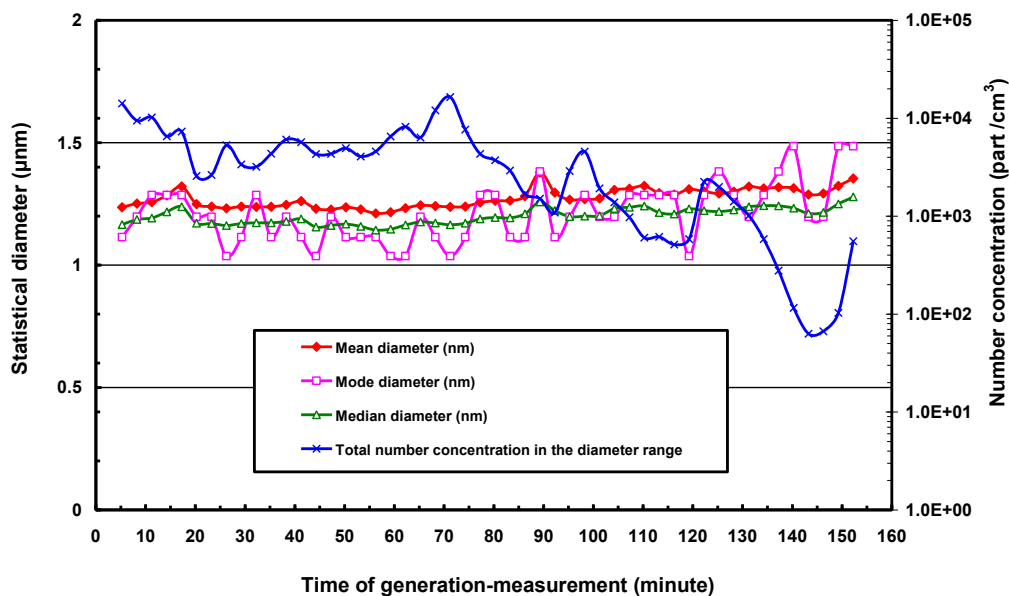
b)

Figure 5. Evolution of the normalized number concentration ($C / C_{t=0}$) of airborne particles measured by SMPS (a) and by APS (b) with a by-pass flow rate of 8 L/min with the different agitation speed configuration: 1500 and 2500 rpm.

Figure 6 presents the evolution of the statistical diameters of the number size distribution (mean, mode and median diameter) and the total number concentration measured by SMPS using diffusion correction (a) and measured by APS (b) during a continuous generation of 150 minutes with TiO₂ nanopowder NM105.



a)



b)

Figure 6. Evolution of the statistical diameters of the number size distribution (mean, mode and median diameter) and the number concentrations number concentrations of airborne particles measured by SMPS using diffusion correction (a) and measured by APS (b) during a continuous generation of 150 minutes with NM105.

During this study, two experimental set-ups were implemented at LNE with the PA100S generator in order to find the optimized instrumental parameters to generate a stable aerosol from the dry aerosolization of the NM 105 powder. In this way, “air nozzle – powder surface” distances of 10 and 12.5 cm were tested. Figure 7 (a to d) present the average number and mass concentrations for APS and SMPS measurements over 3.5 hours for the optimized generation process of NM 105 powder using this generator, i.e. with the “air nozzle – powder surface” distance of 12.5 cm. Associated uncertainties correspond to the standard deviation calculated on three repeated experiments.

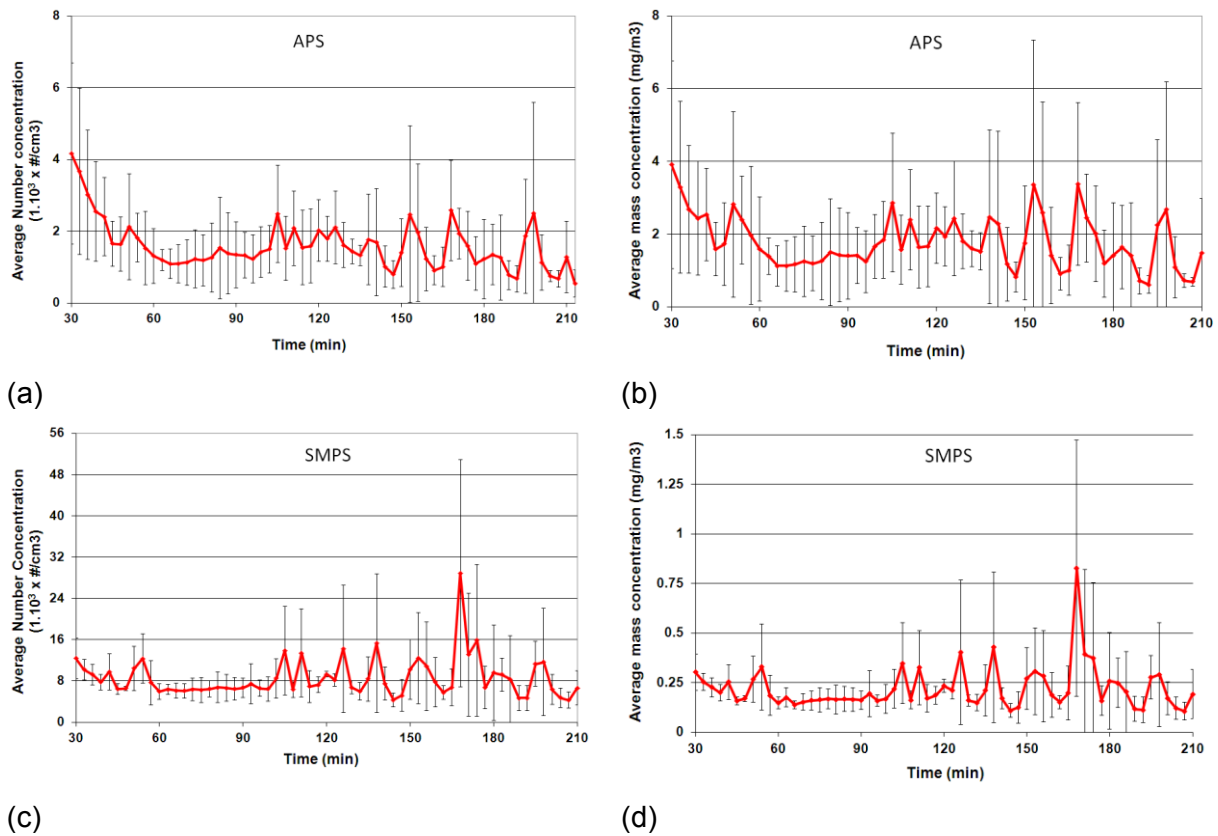


Figure 7. (a)-(c) - Average number concentrations for APS and SMPS measurements, (b)-(d) – average mass concentrations for APS and SMPS measurements, over time (3,5 hours) for the optimized generation process of NM 105 powder using PA100S generator (“air nozzle/powder surface” distance = 12.5 cm). Associated uncertainties correspond to one standard deviation calculated on three experiments.

4.2.1.3 Conclusions

In the absence of optimized parameters, the use of the PA100S leads to unstable aerosols. It was demonstrated that the aerosol is bimodal: 1 mode around 300-500 nm, and another mode around 1-1.5 μm . In addition, the total number concentration of the aerosols produced was found to decrease with time over 150 minutes.

When optimized parameters are applied, better aerosol stability is observed, with acceptable deviations between three repeated experiments.

4.2.2 Dry-based method – Rotating Brush Generator (PALAS RBG1000)

The objective of the use of this generator, which has been widely described, was to provide inter-comparison data between the different NM tested. For some of them, identical measurements were performed in both LNE and INRS.

4.2.2.1 Description of the experimental setup

Figure 8 is a schematic of the experimental setup.

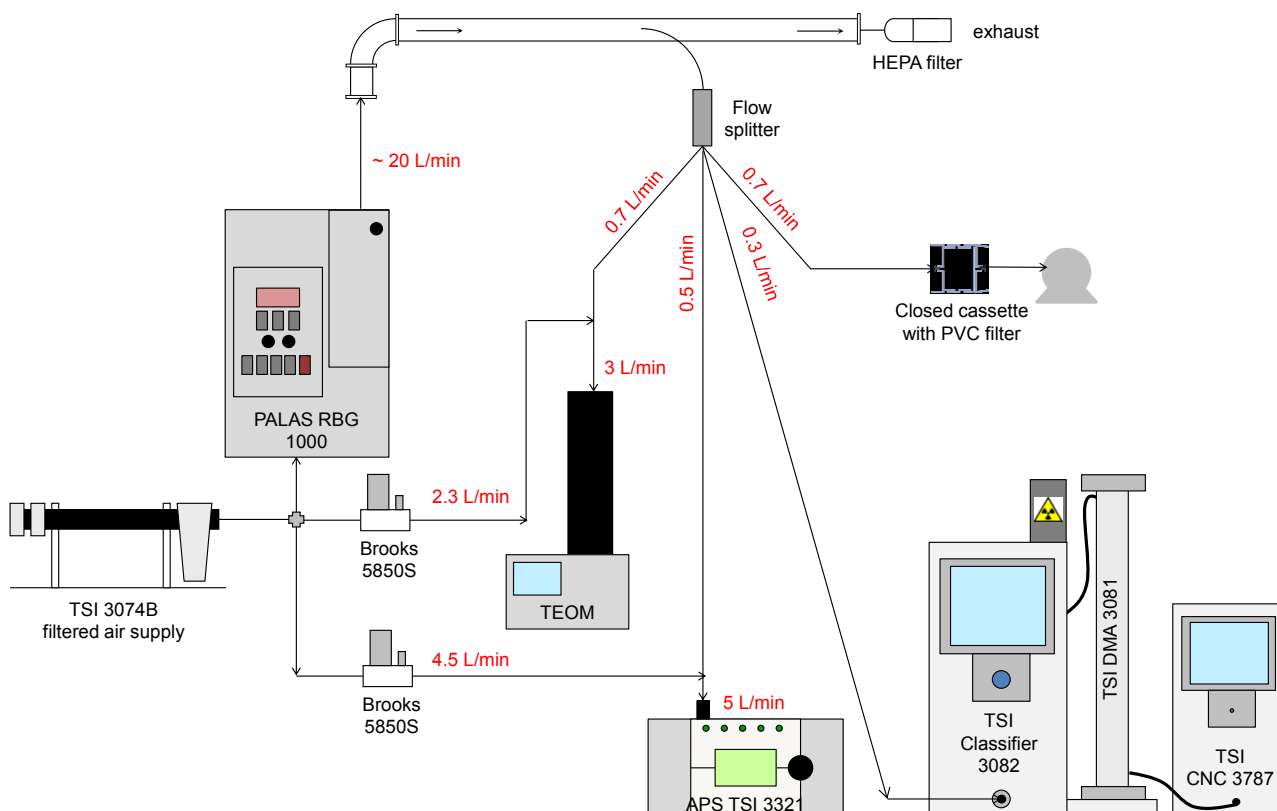


Figure 8. Schematic of the experimental setup involving the Rotating Brush Generator.

The amount of powder introduced in the cylinder varied between 0.5 g to 2 g, depending on the powder considered. For some of them (with very low densities), the powder was manually tapped to reach 0.5 mg within the cylinder.

The initial position of the piston was set to 65 mm. In a first step, the piston was elevated at high speed until the piston position reaches 30 mm. The RBG was then operated under 1 bar inlet pressure, with a rotation of 1200 rpm and an elevation speed of 4 mm/h. It should be specified that no further action of the operator was required during the generation. Thus, the packing of the powder due to the elevation of the piston leads, for some cases, to an increase of the aerosolized amount with time. This is observed for e.g. NM105.

The aerosol characterization was based on the real-time measurement of airborne particle number size distribution (SMPS + APS), associated with its mass concentration (TEOM). Samples with a closed-face cassette were simultaneously taken for further off-line gravimetric analysis. For each powder, two runs were reproduced. The data presented in this report correspond to the time-resolved number and mass concentrations, as well as the averaged number size distributions.

The characterization of a nano-object is a complex process, due to the large number of parameters to be taken into consideration, and to the tendency of these parameters to change during the product's life cycle. LNE has been addressing these nano-object characterization issues for several years and has developed a dedicated platform which constitutes the national metrological reference for nanoscale characterization. The CARMEN platform thus provides, in a clean room and controlled atmosphere environment, all the measurement instruments required for complete characterization of a nano-object (AFM, SEM-EDX, DLS, zeta potential, BET, XRD). A metrological AFM, specific to LNE, completes the CARMEN platform and ensure direct metrological traceability for dimensional measurements, the only means of guaranteeing the reliability and comparability of the measurement results obtained. The fact that these various devices are available in a clean room setting avoids any risk of sample contamination during handling and transition from one instrument to the next.

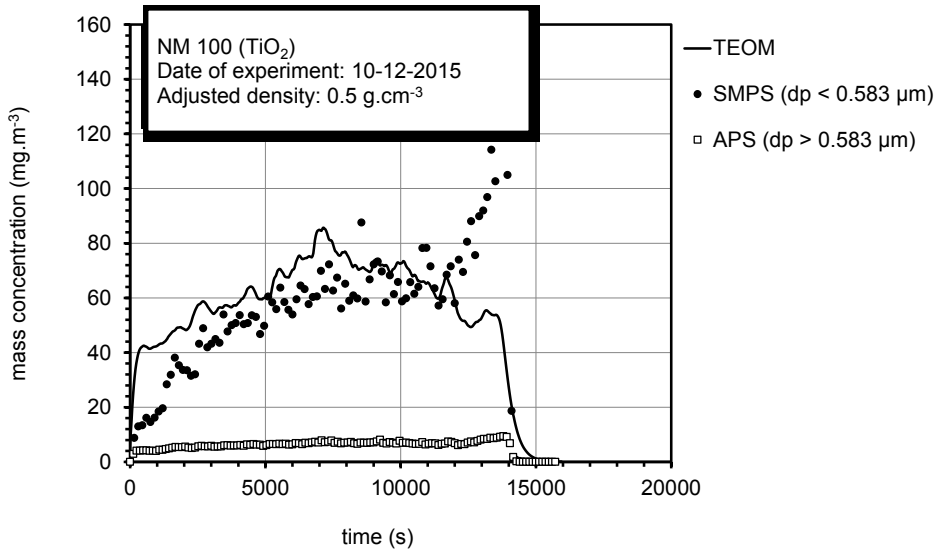
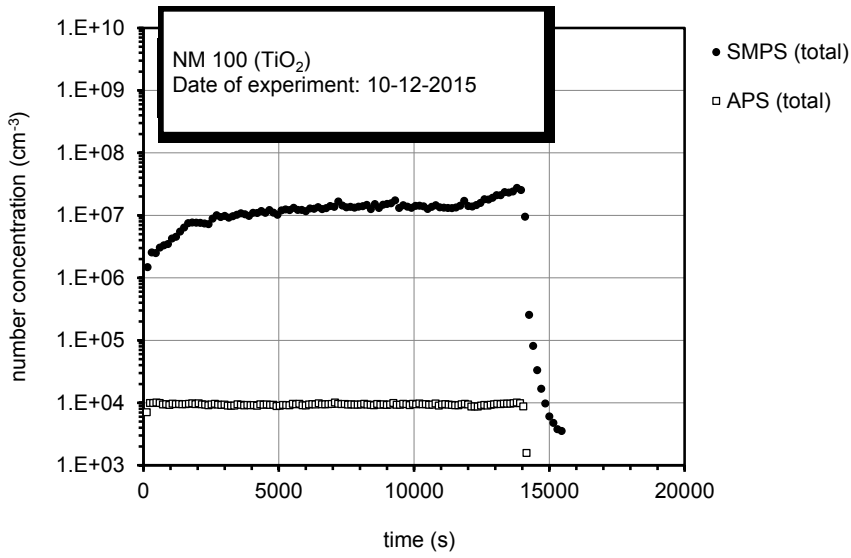
Therefore, SEM analysis were performed on several powders sampled on filter downstream the aerosolisation process using the RBG 1000 generator. When available, SEM images are also provided in the next paragraphs.

4.2.2.2 Case of titanium dioxide nanomaterials

Four different titanium dioxides (NM 100, 101, 103 and 105) were investigated.

For each NM, figures present 1) time series of the number concentrations obtained by SPMS and APS; 2) time series of the mass concentration as measured by TEOM and calculated by SPMS and APS; 3) number size distribution obtained by SMPS and APS; 4) SEM photography of collected particles.

➤ NM100 (LNE)



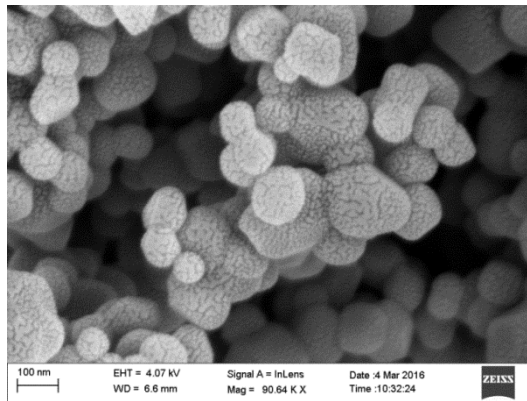
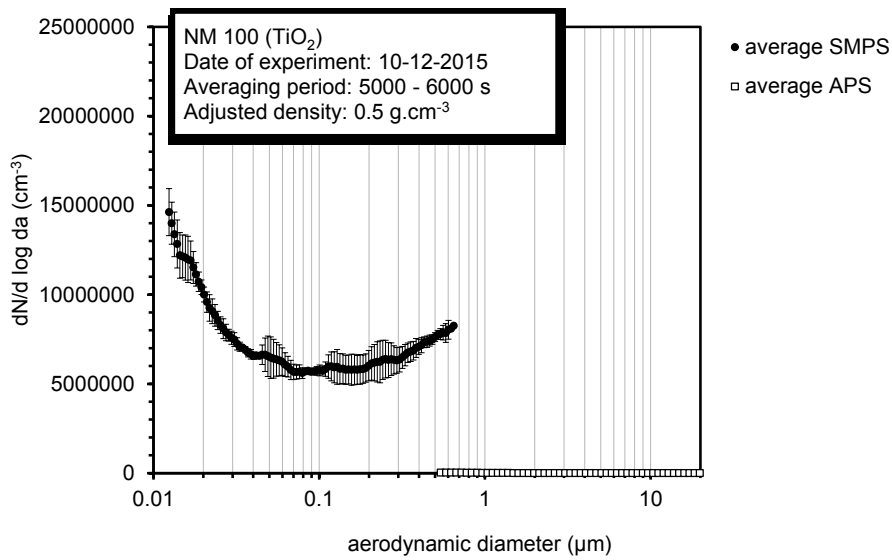
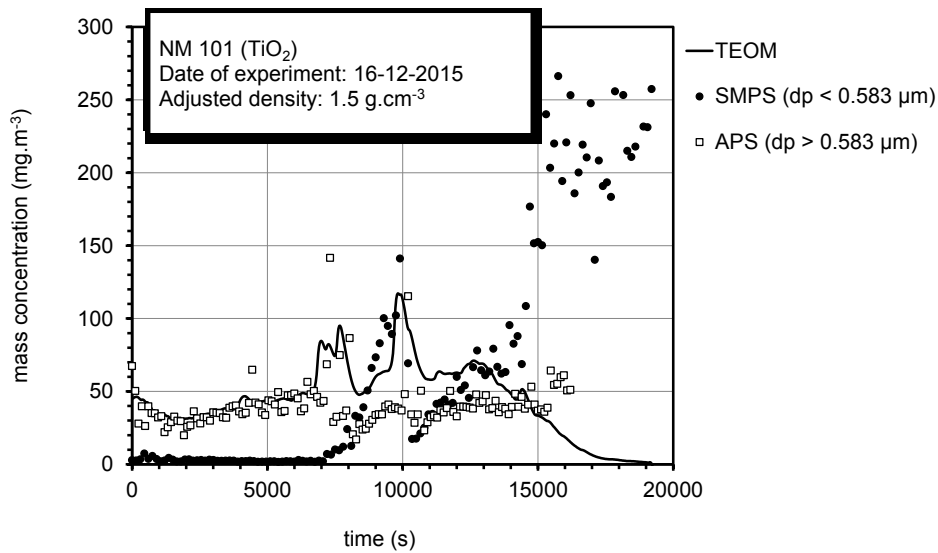
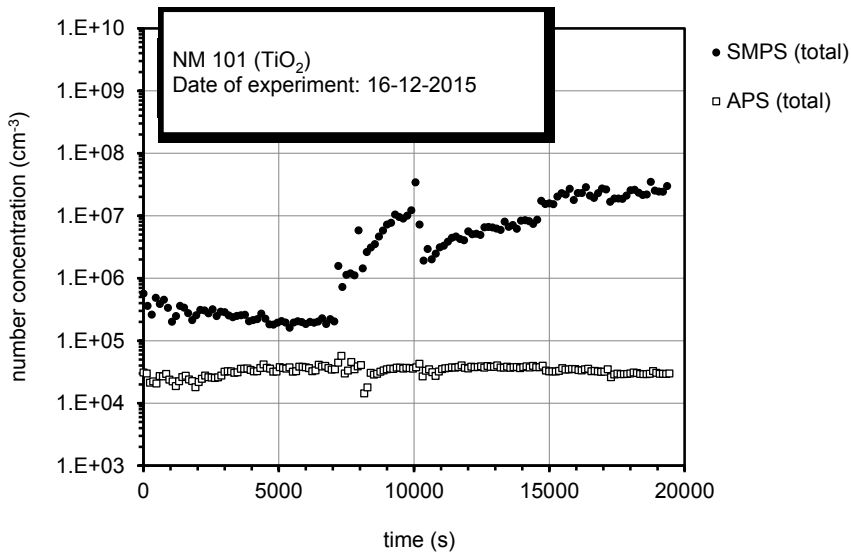


Figure 9. Experimental data for NM 100 by LNE.

Data from Figure 9 indicates that the aerosol produced from NM100 powder is very stable with time (over 4 hours), highly concentrated in number ($> 10^7 \text{ cm}^{-3}$) as well as in mass (around 60 mg.m^{-3}). The corresponding number size distribution, although difficult to interpret, demonstrates that most airborne particles are likely below $1 \mu\text{m}$.

➤ NM101 (LNE)



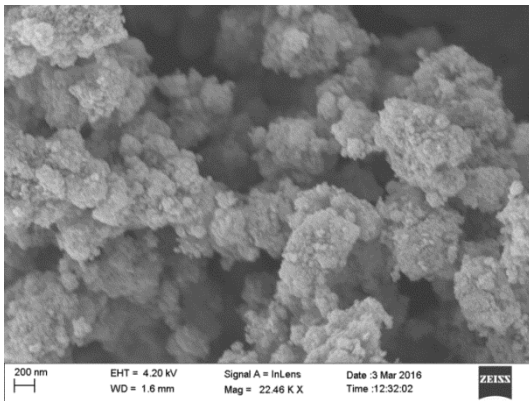
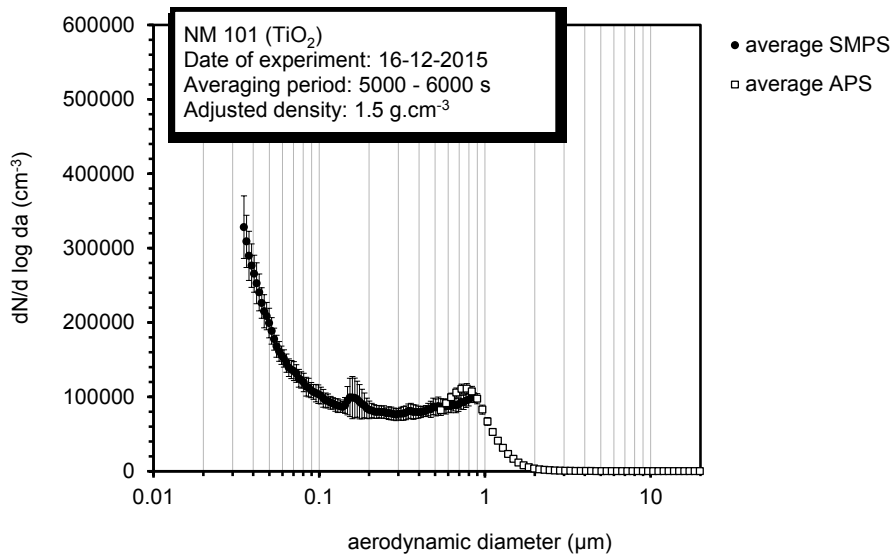
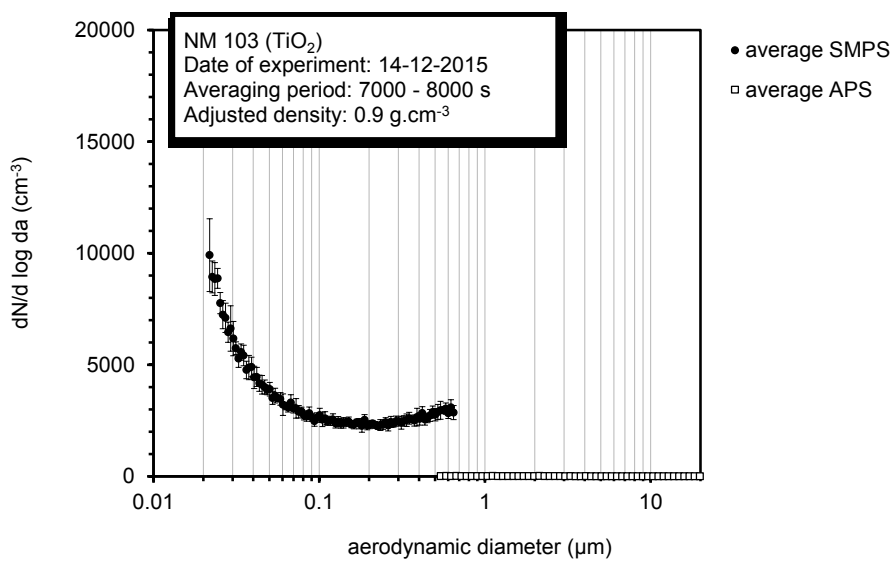
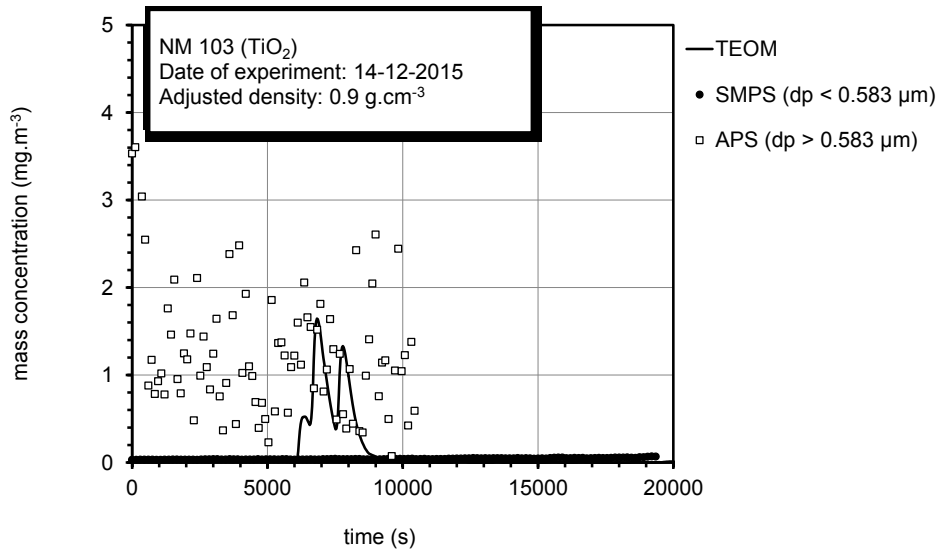
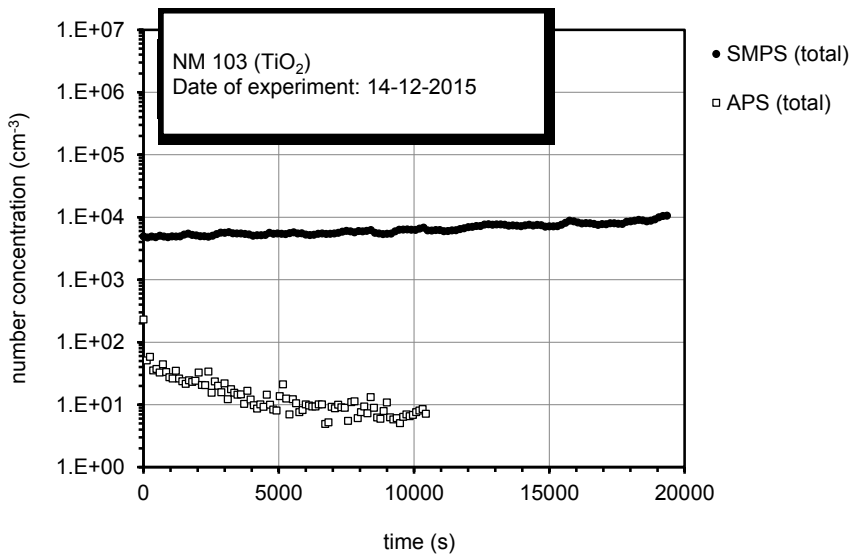


Figure 10. Experimental data for NM 101 by LNE.

Data from Figure 10 indicates that the aerosol produced from NM101 powder is quite stable with time in its micron part, and less stable concerning the submicron part. Once established (above 10000 seconds), the aerosol is highly concentrated in number ($\sim 10^7 \text{ cm}^{-3}$) as well as in mass (around 60 mg.m^{-3}). The corresponding number size distribution, although difficult to interpret, demonstrates that most airborne particles are below $1 \mu\text{m}$; it presents a first mode below 30 nm , and a second mode around $0.7\text{-}0.8 \mu\text{m}$.

➤ NM103 (LNE)



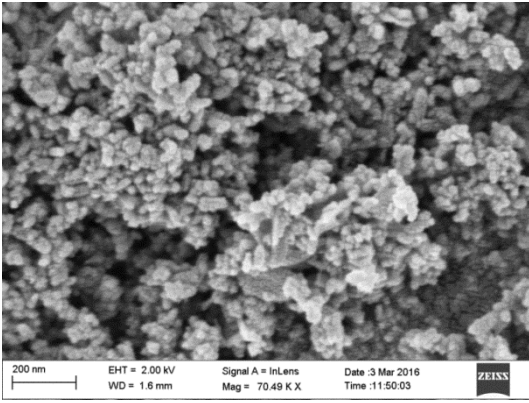
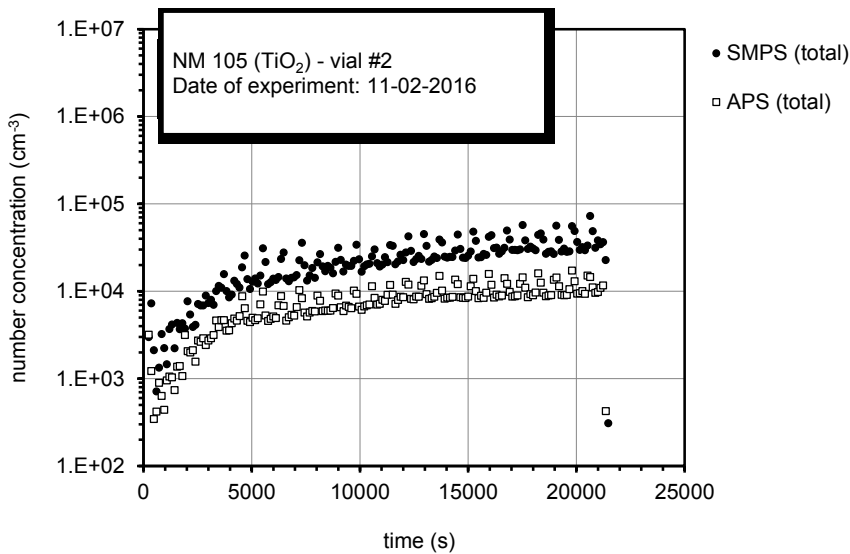


Figure 11. Experimental data for NM 103 by LNE.

Data from Figure 11 indicates that the aerosol produced from NM103 powder is quite stable with time (over 4 hours), not very concentrated in number ($\sim 10^4 \text{ cm}^{-3}$), very low in terms of mass concentration ($< 2 \text{ mg.m}^{-3}$). The corresponding number size distribution, although difficult to interpret, demonstrates that airborne particles are all below $1 \mu\text{m}$.

➤ NM105 (INRS)



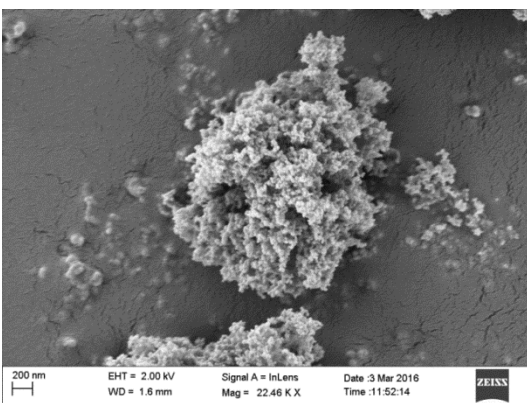
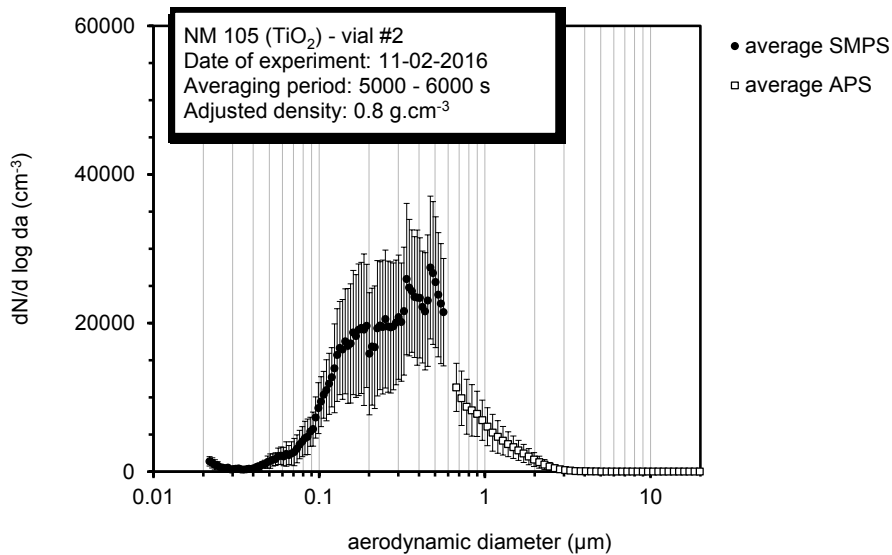
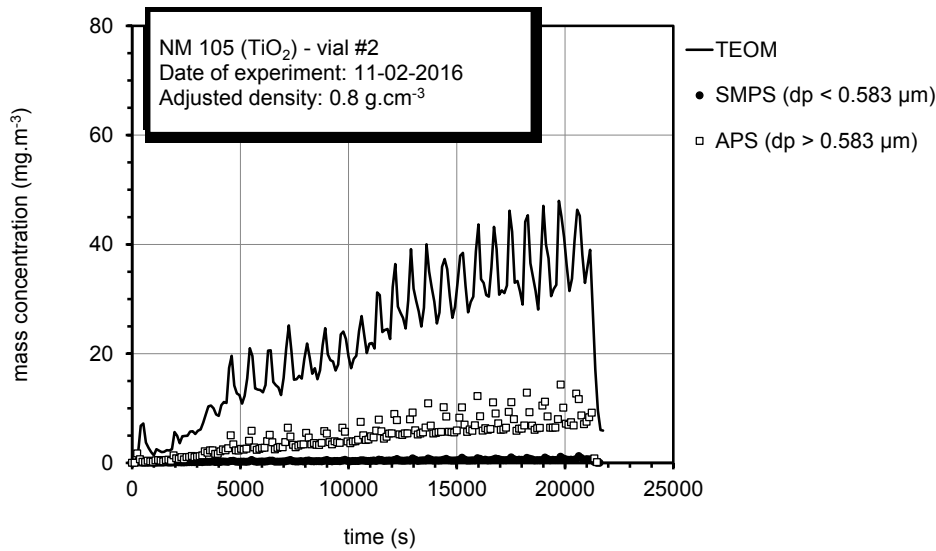


Figure 12. Experimental data for NM 105 by INRS.

Data from Figure 12 indicates that the aerosol produced from NM105 powder is increasing in terms of both number and mass concentrations. The aerosol is quite concentrated in number ($\sim 10^4 \text{ cm}^{-3}$), highly concentrated in mass (around 30 mg.m^{-3}). The corresponding number size distribution demonstrates that most airborne particles are below $1 \mu\text{m}$; it presents a mode around $0.3\text{-}0.5 \mu\text{m}$.

➤ NM105 (LNE)

No TEOM data and SMPS data to be considered with caution due to inappropriate measurement parameters.

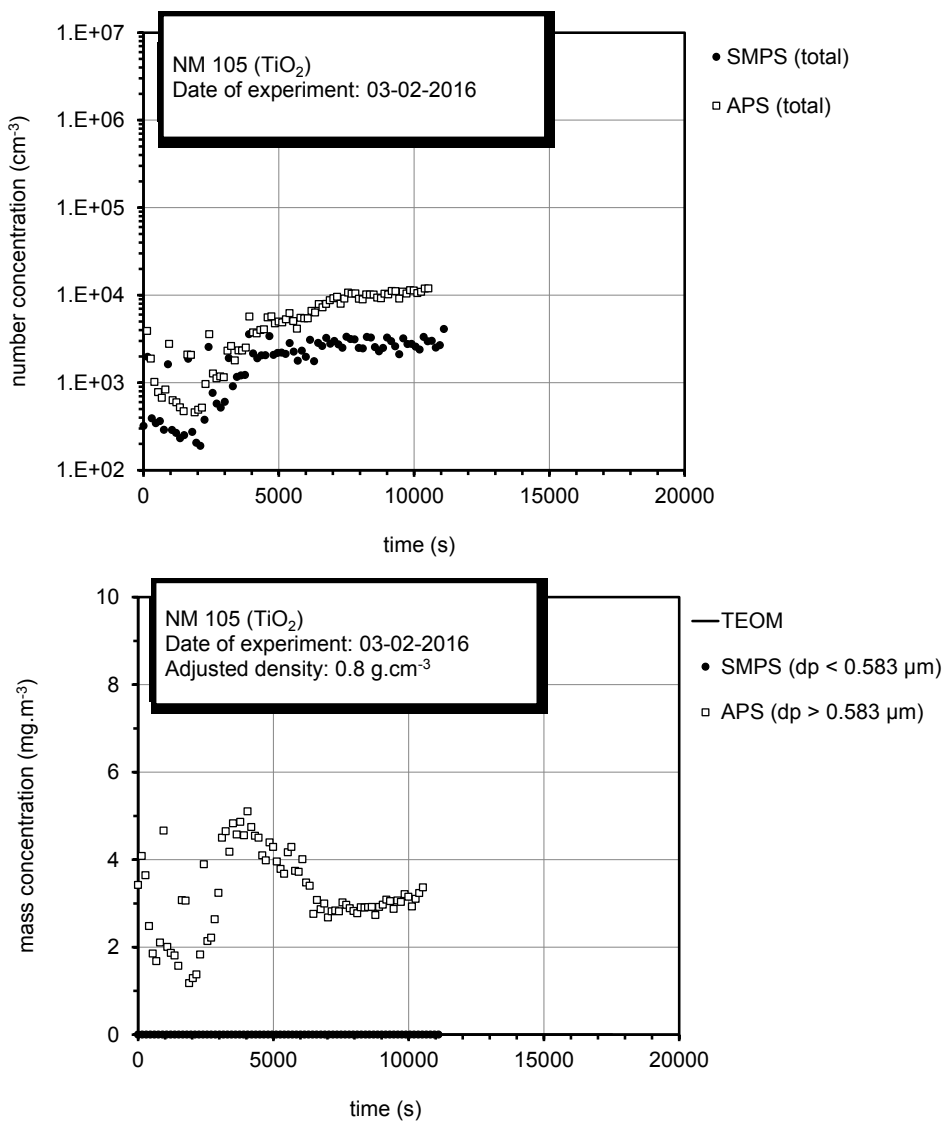


Figure 13. Experimental data for NM 105 by LNE.

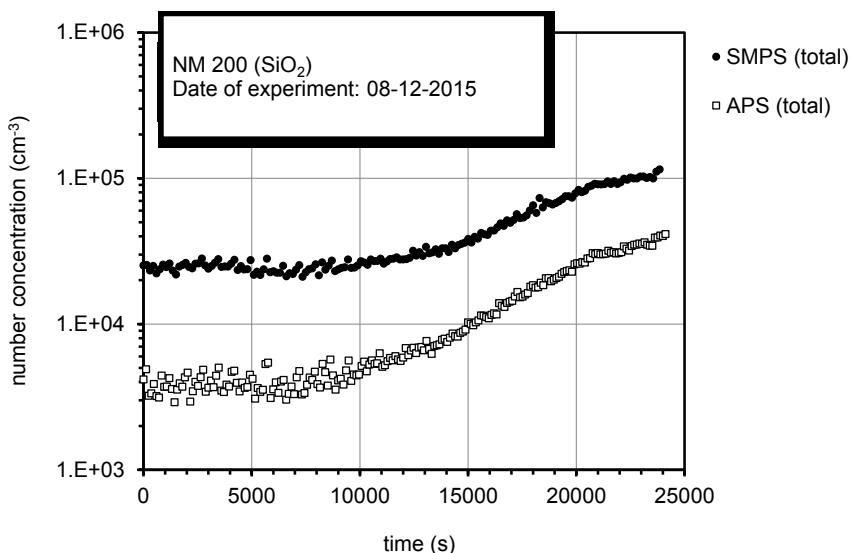
In the absence of relevant data, no further conclusions can be drawn. Figure 13 suggests that the number concentration of airborne particles is quite stable after 5000 seconds, around 10^4 cm^{-3} for APS data and $3 \cdot 10^3 \text{ cm}^{-3}$ for SMPS data, respectively. The corresponding mass concentration is around $3 \text{ mg} \cdot \text{m}^{-3}$, based on APS calculations.

4.2.2.3 Case of silica nanomaterials

Two amorphous silica were investigated: NM 200, NM 203.

For each NM, figures present 1) time series of the number concentrations obtained by SPMS and APS; 2) time series of the mass concentration as measured by TEOM and calculated by SPMS and APS; 3) number size distribution obtained by SMPS and APS; 4) SEM photography of collected particles.

➤ NM200 (LNE)



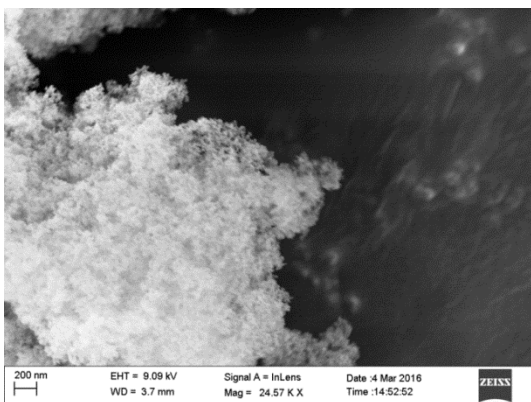
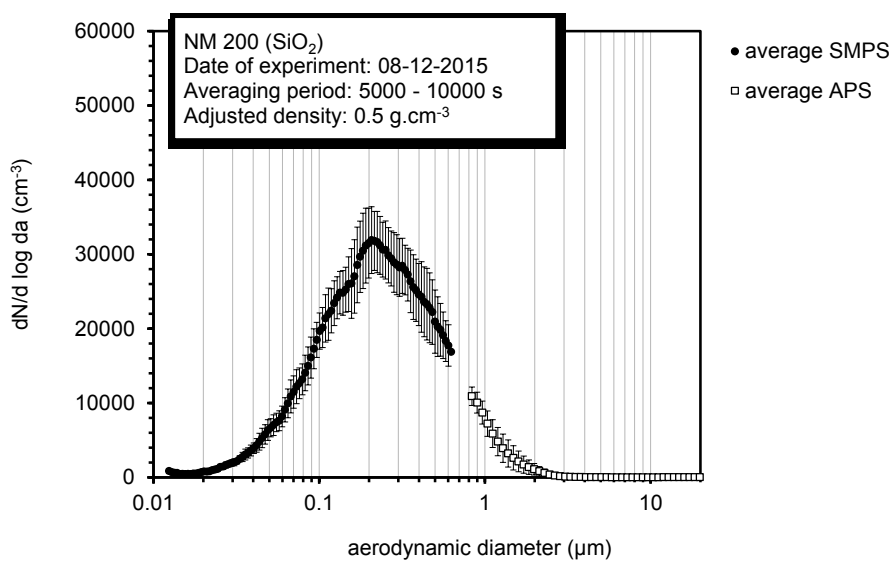
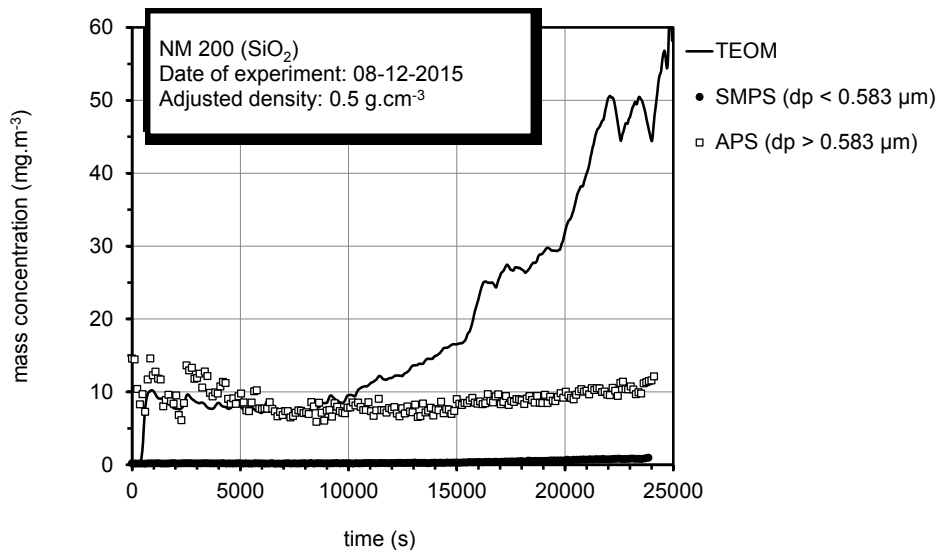
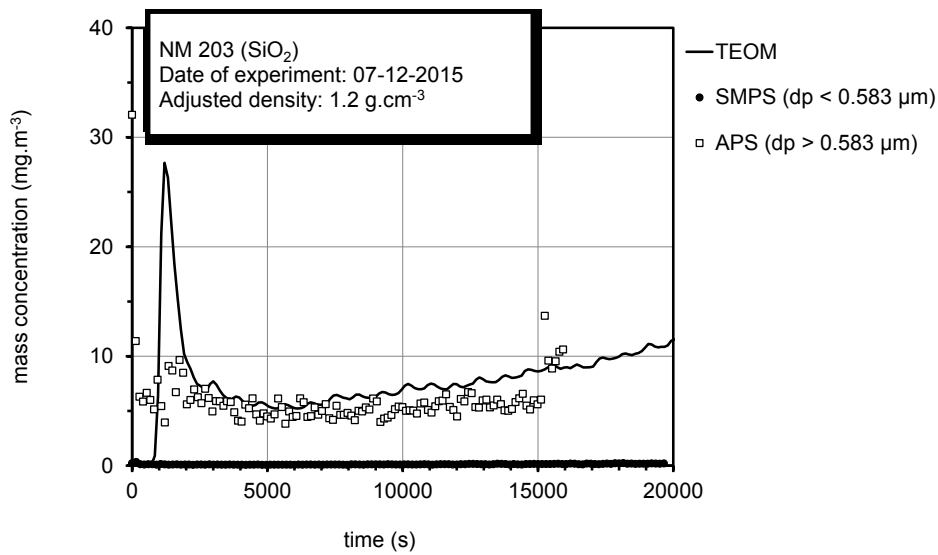
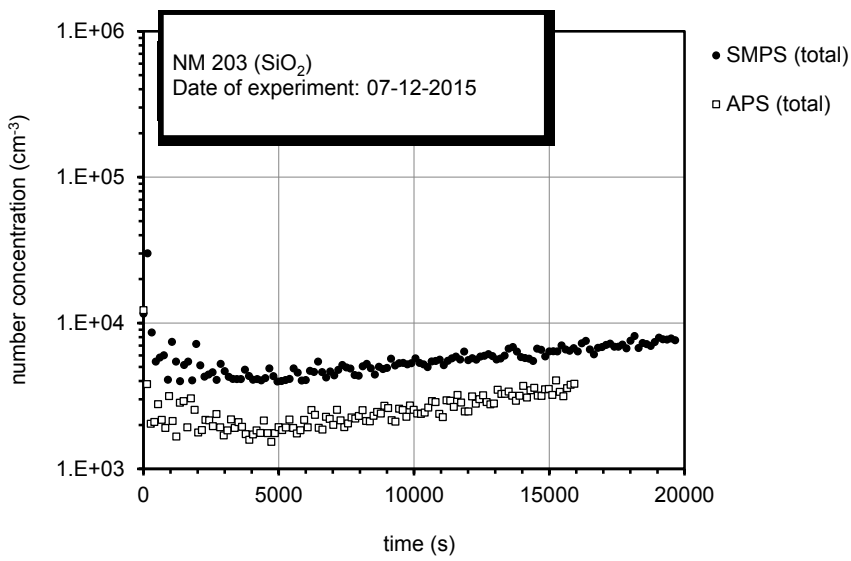


Figure 14. Experimental data for NM 200 by LNE.

Data from Figure 14 indicate that the aerosol produced from NM200 powder is first stable during 10000 second, and then starts increasing in terms of both number and mass concentrations. The aerosol is quite concentrated in number ($\sim 10^4 \text{ cm}^{-3}$), quite concentrated in mass (around 8 mg.m^{-3}). The corresponding number size distribution demonstrates a mode around $0.2 \mu\text{m}$.

➤ NM 203 (LNE)



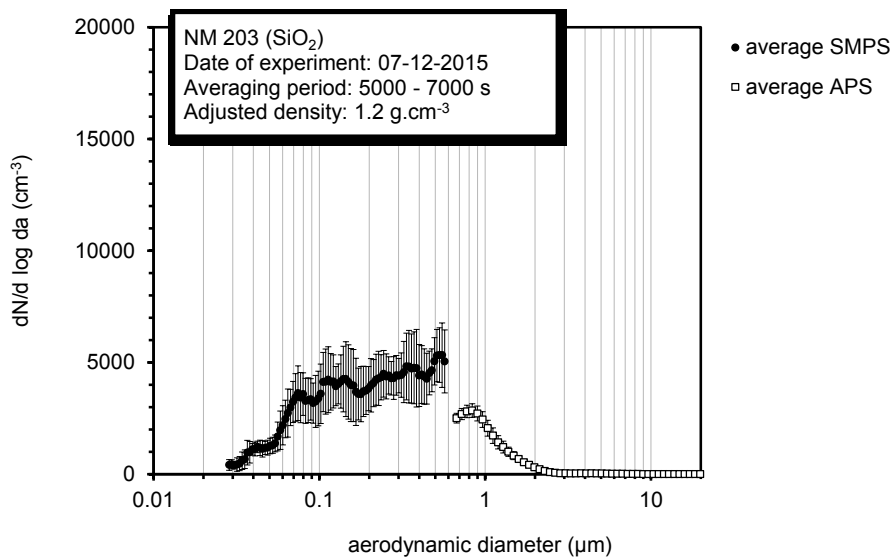
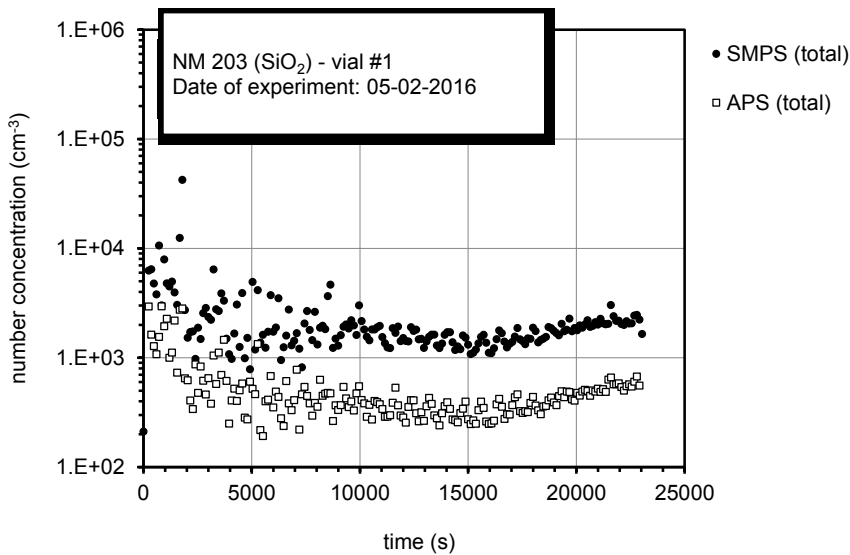


Figure 15. Experimental data for NM 203 by LNE.

Data from Figure 15 indicate that the aerosol produced from NM203 powder is quite stable during 15000 second, with a slight increase in terms of both number and mass concentrations. The aerosol present a low concentration in number ($< 10^4$ cm⁻³), and is quite concentrated in mass (around 5-7 mg.m⁻³). The corresponding number size distribution suggests the existence of a mode around 0.2-0.5 μm.

➤ NM203 (INRS)



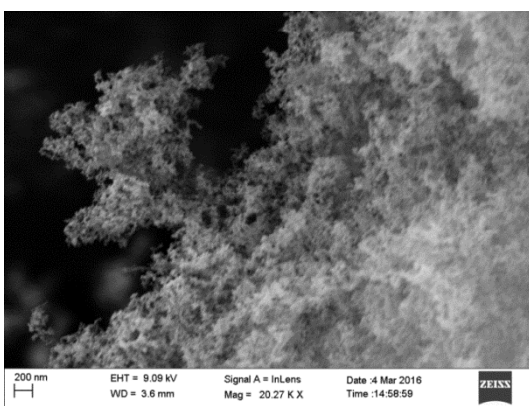
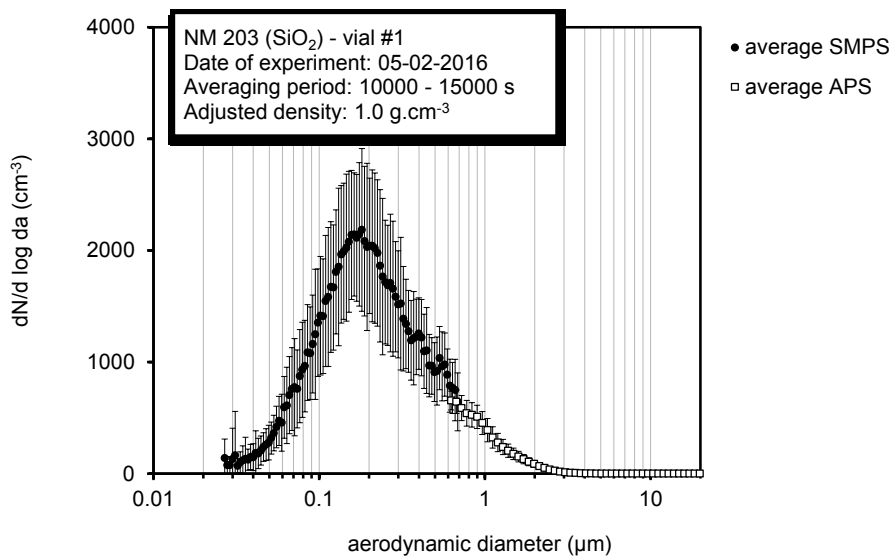
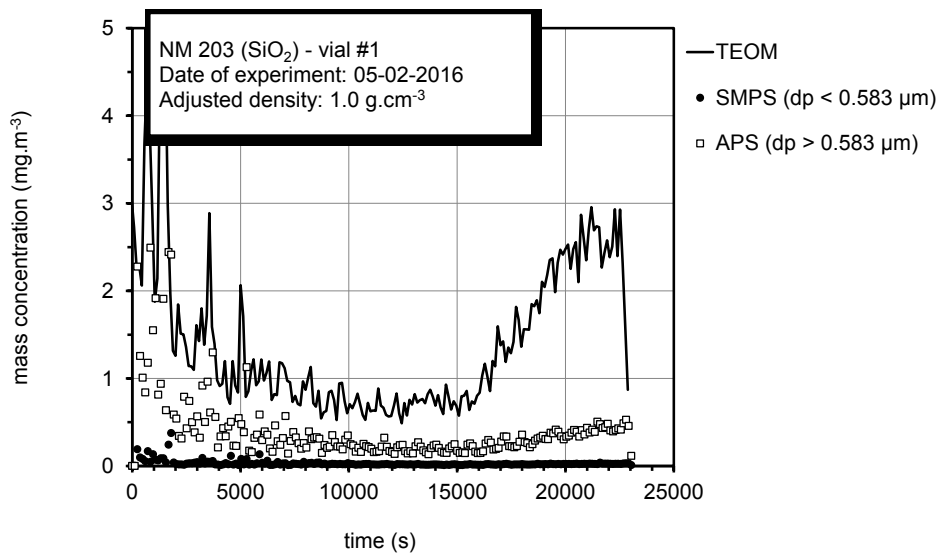


Figure 16. Experimental data for NM 203 by INRS.

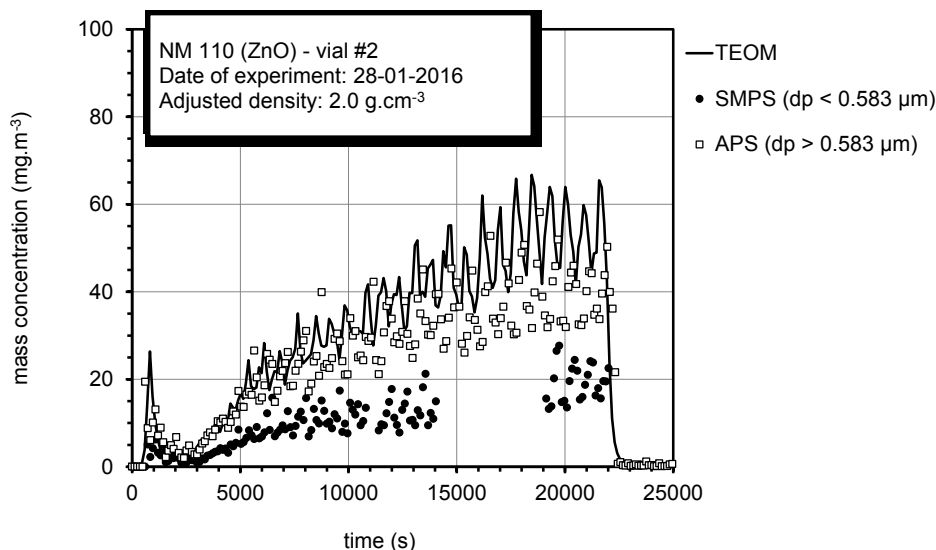
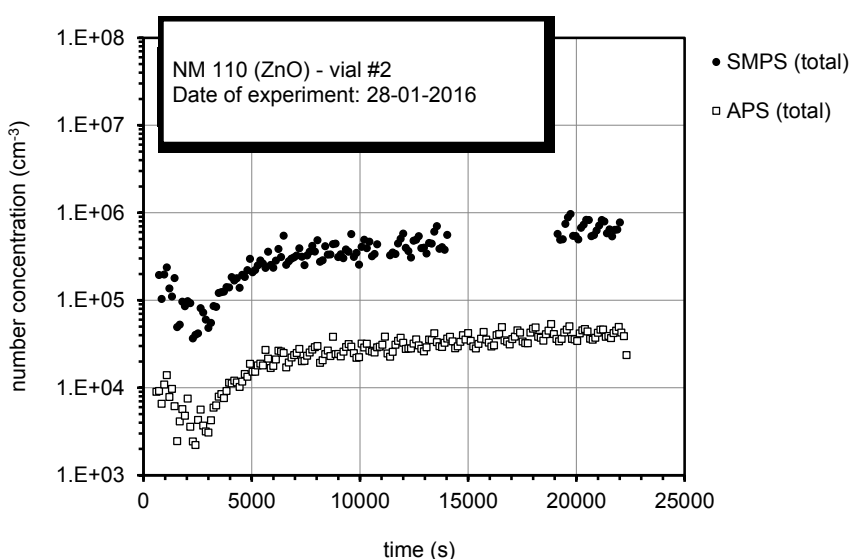
Figure 16 indicates that the aerosol produced from NM203 powder is quite stable before 15000 second, starting then to slightly increase in terms of mass concentration. The aerosol presents a very low concentration in number ($< 10^4 \text{ cm}^{-3}$), as well as in mass ($< 1 \text{ mg.m}^{-3}$). The corresponding number size distribution highlights a mode around $0.2 \mu\text{m}$.

4.2.2.4 Case of other oxide nanomaterials

In addition to TiO_2 and SiO_2 , other NMs have been investigated. There are: NM110 (ZnO), NM212 (CeO) and NM220 (BaSO_4).

For each NM, figures present 1) time series of the number concentrations obtained by SPMS and APS; 2) time series of the mass concentration as measured by TEOM and calculated by SPMS and APS; 3) number size distribution obtained by SMPS and APS; 4) SEM photography of collected particles.

➤ NM110 (INRS)



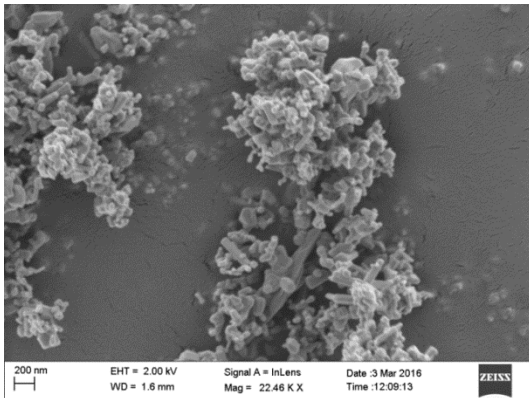
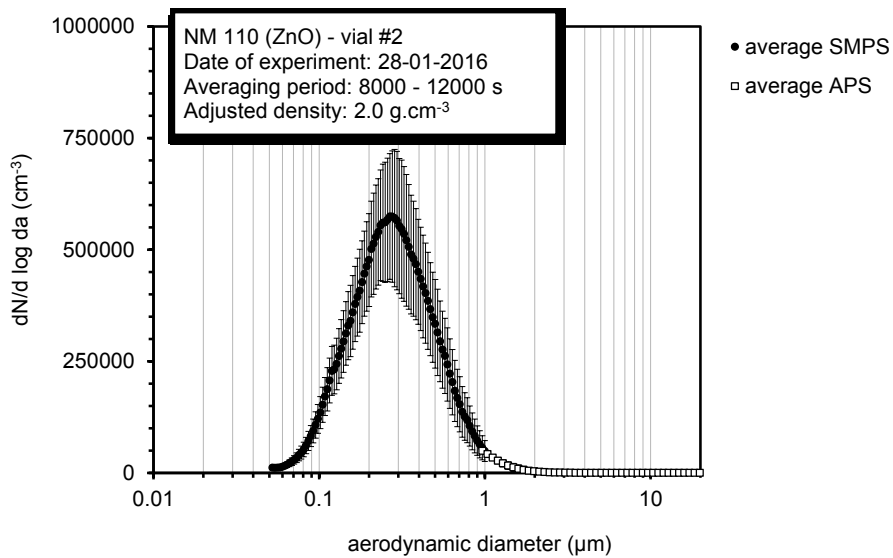
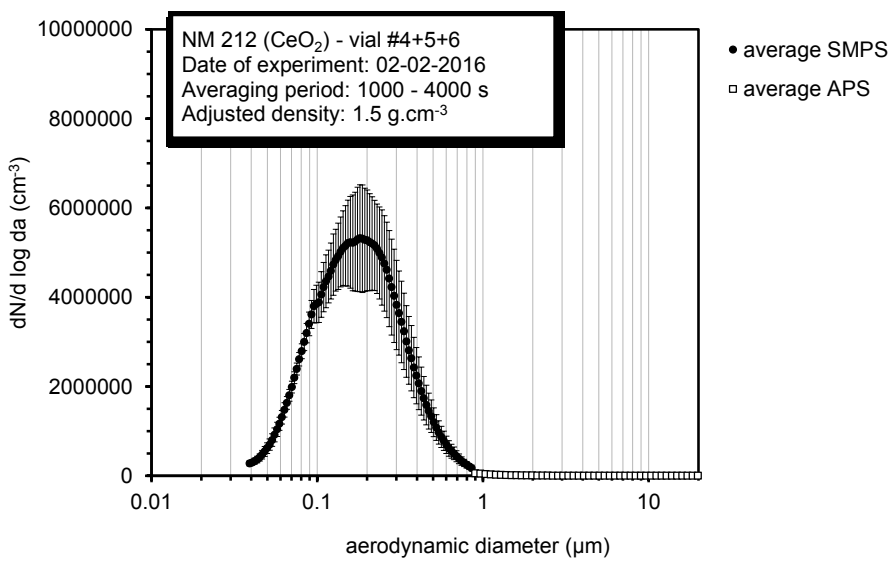
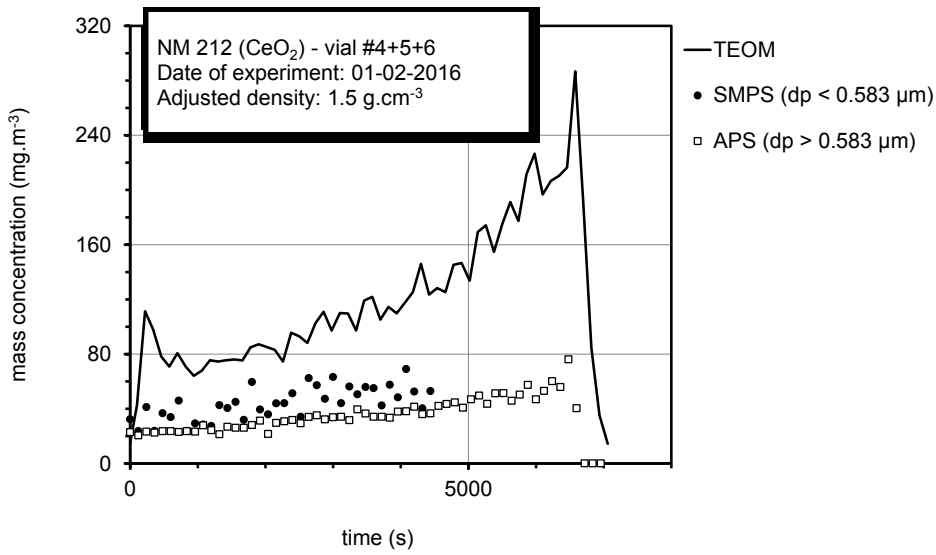
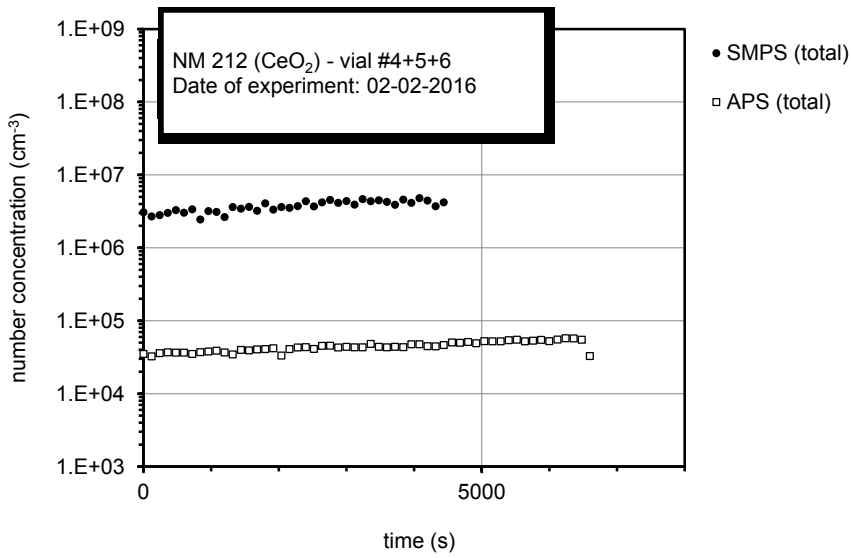


Figure 17. Experimental data for NM 110.

Figure 17 indicates that the aerosol produced from NM110 powder is continuously increasing with time in terms of both number and mass concentrations. The aerosol presents a very high concentration in number ($> 10^5 \text{ cm}^{-3}$), and a highly variable mass concentration, ranging from less than 5 to 60 mg.m^{-3} in 5 hours. The corresponding number size distribution highlights a mode around 0.2-0.3 μm . Almost no particle above 1 μm is observed.

➤ NM212 (INRS)



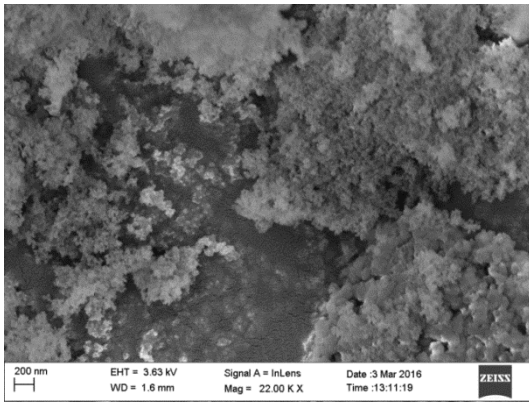
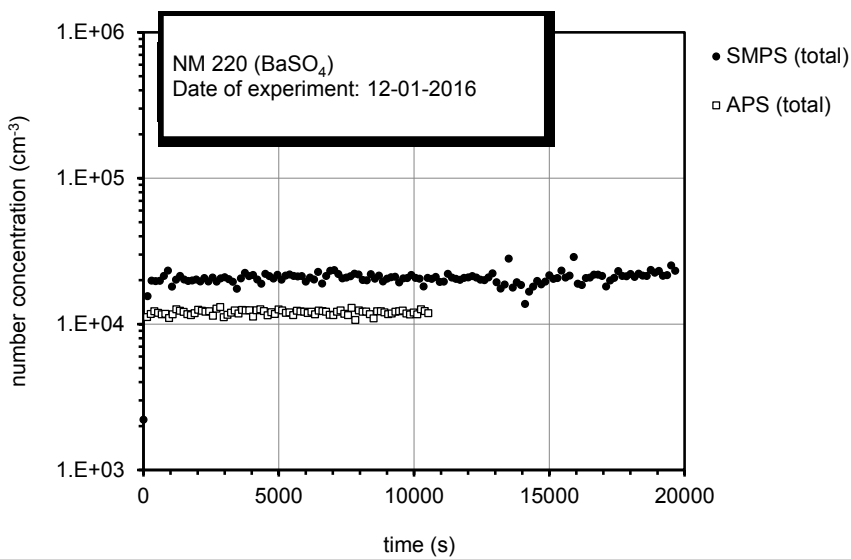


Figure 18. Experimental data for NM 212.

Figure 18 shows that the aerosol produced from NM212 powder is quite stable with time for ~ 5000 seconds. The aerosol presents a very high concentration in both number ($> 10^6 \text{ cm}^{-3}$) and in mass ($> 80 \text{ mg.m}^{-3}$) concentration. The corresponding number size distribution highlights a mode around $0.2 \mu\text{m}$. No particle above $1 \mu\text{m}$ is observed.

➤ NM220 (LNE)



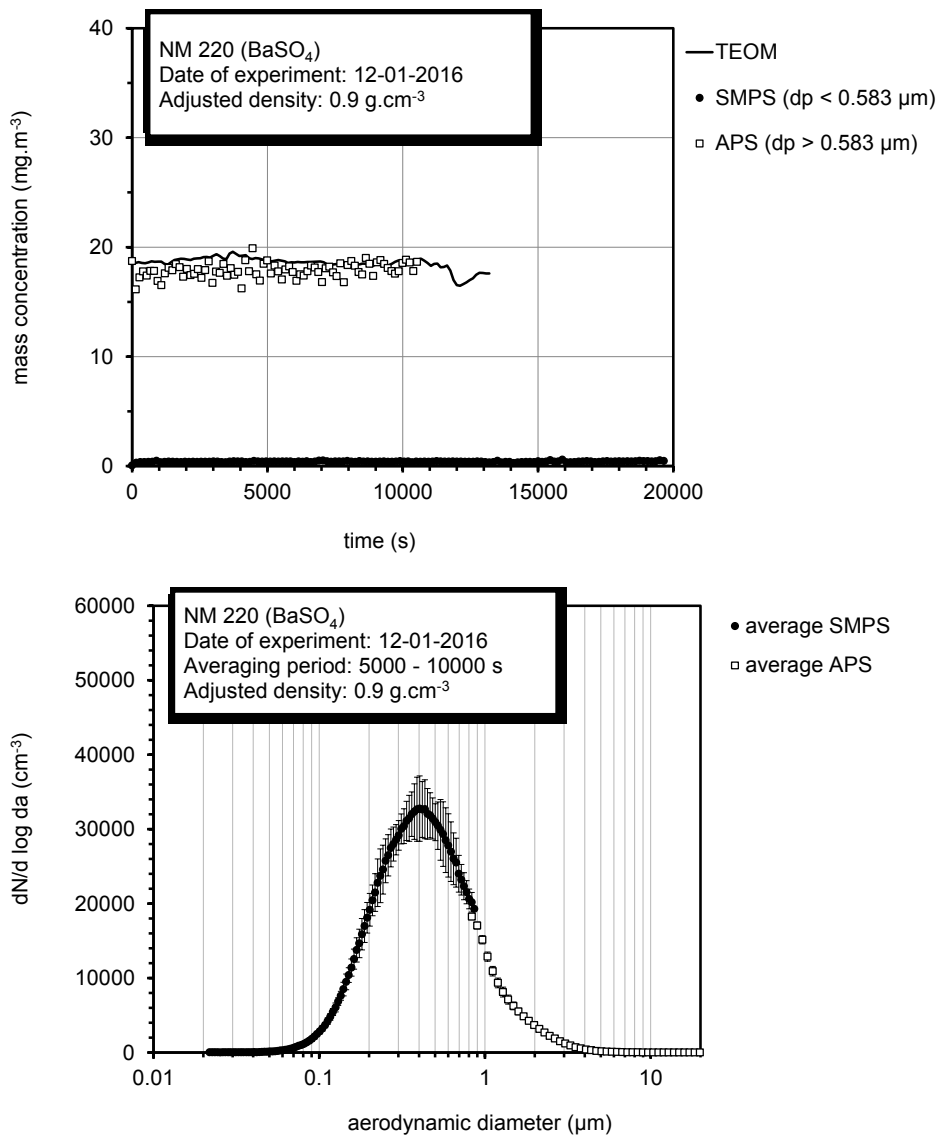
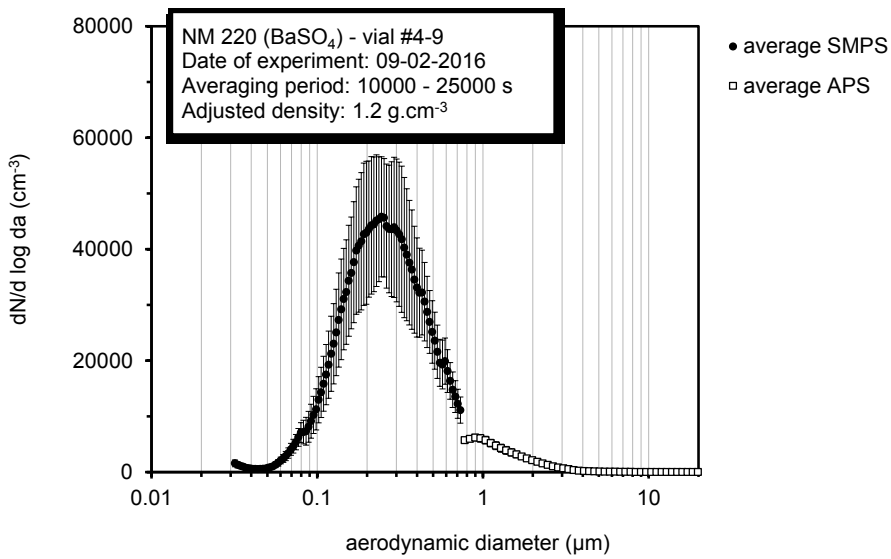
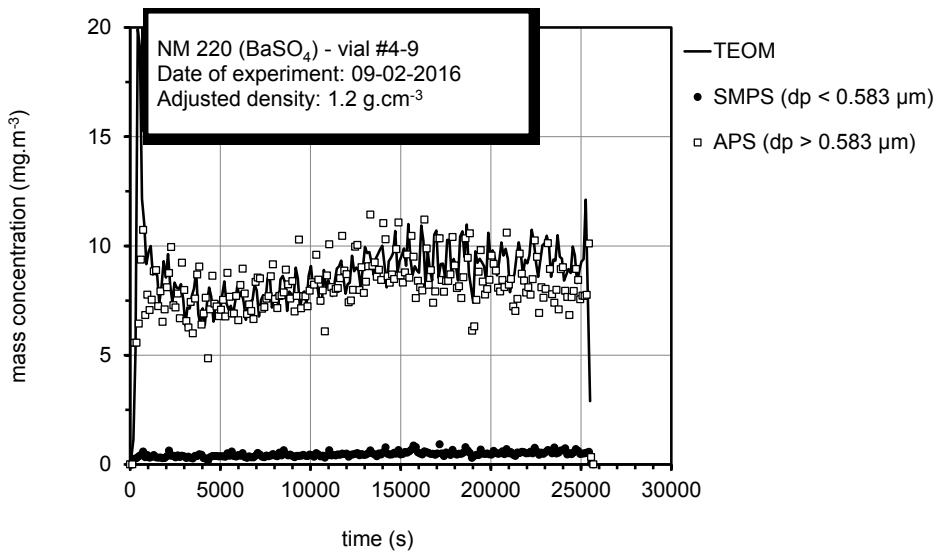
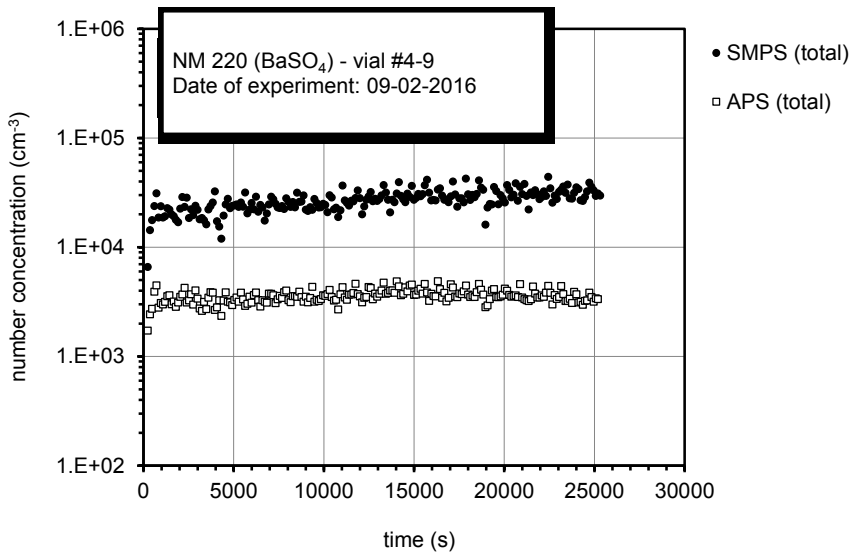


Figure 19. Experimental data for NM 220 by LNE.

It can be observed from Figure 19 a very high stability of the aerosols produced from NM220 powder over time. The high number concentration ($> 10^4 \text{ cm}^{-3}$ for both SMPS and APS) and mass concentration ($\sim 18 \text{ mg.m}^{-3}$) is associated with a constant number size distribution which presents a mode around $0.4 \mu\text{m}$.

➤ NM 220 (INRS)



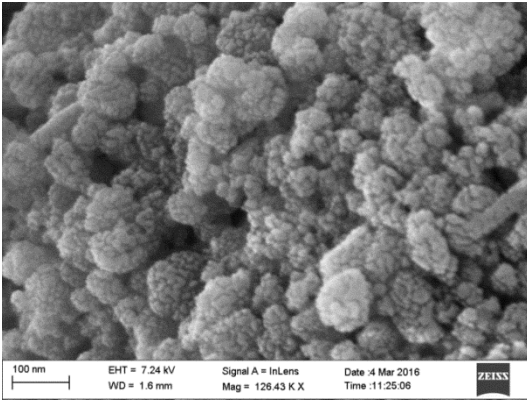


Figure 20. Experimental data for NM 220 by INRS.

Again, it can be observed from Figure 20 a very high stability of the aerosols produced from NM220 powder over time. The high number concentration ($> 2 \cdot 10^4 \text{ cm}^{-3}$ for SMPS and $> 3 \cdot 10^3 \text{ cm}^{-3}$ APS) and quite high mass concentration ($\sim 8 \text{ mg} \cdot \text{m}^{-3}$) is associated with a constant number size distribution which presents a mode around $0.3 \mu\text{m}$.

4.2.2.5 Repeatability of aerosol generation according to the mass concentrations

The use of the closed-face cassette in parallel with real-time devices led to the determination of the average mass concentrations, as shown in Figure 21.

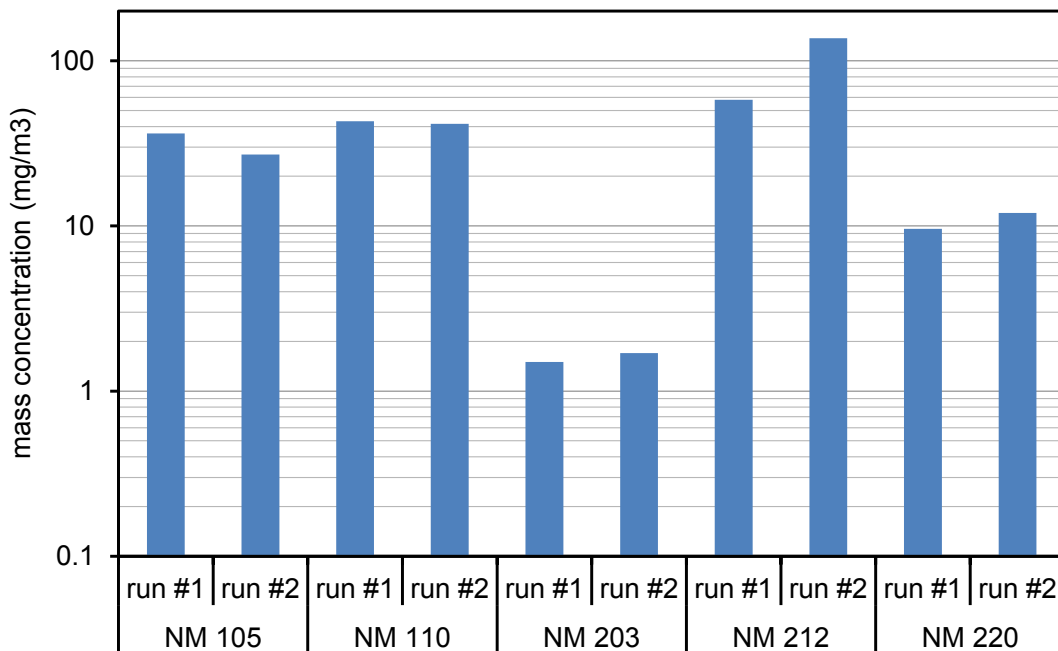


Figure 21. Average mass concentrations stemming from off-line gravimetric analysis.

It can be observed from Figure 21 a satisfying repeatability of the mass concentrations obtained by subsequent gravimetric analysis, whatever the substance considered. The average coefficient of variation

observed is 20%, ranging from 3% for NM110 to 60% for NM212. A quite large span can also be highlighted from Figure 21, covering 2 orders of magnitude from $\sim 1 \text{ mg.m}^{-3}$ to $\sim 100 \text{ mg.m}^{-3}$.

4.2.2.6 Conclusions

Based on this large set of experimental data stemming from time-resolved metrology, the following Table 2 can be drawn to gather information relative to the different NM investigated.

Table 2. Summary of aerosols obtained in tests carried out using RBG.

NM	Institute	Number concentration (cm^{-3})	Mass concentration (mg.m^{-3})	Number size distribution
100	LNE	$\sim 10^7$ stable	~ 60 quite stable	all $< 1 \mu\text{m}$, mode likely $< 10 \text{ nm}$
101	LNE	$\sim 2 \cdot 10^7$ stable after 10000 s	~ 60 quite stable	2 modes: $< 30 \text{ nm}$ and $\sim 0.7\text{-}0.8 \mu\text{m}$
103	LNE	$\sim 10^4$ quite stable	< 2	all $< 1 \mu\text{m}$, mode likely $< 30 \text{ nm}$
105	INRS	$\sim 5 \cdot 10^4$ increasing with time	~ 30	1 mode $\sim 0.3\text{-}0.5 \mu\text{m}$
105	LNE	$\sim 10^4$ Stable over 20000 s	~ 3 (APS-based)	NA
200	LNE	$\sim 3 \cdot 10^4$ stable over 10000 s, increasing afterwards	~ 8 , up to ~ 60	1 mode $\sim 0.2 \mu\text{m}$
203	LNE	$< 10^4$ stable	~ 7	1 mode $\sim 0.2\text{-}0.5 \mu\text{m}$
203	INRS	$< 10^4$ stable	< 1 Stable until 15000 s, increasing afterwards	1 mode $\sim 0.2 \mu\text{m}$
110	INRS	$> 10^5$ increasing with time	from 0 to 60 in 5 hours	all $< 1 \mu\text{m}$, 1 mode $\sim 0.2\text{-}0.3 \mu\text{m}$
212	INRS	$> 10^6$ stable over 5000 s	> 80	1 mode $\sim 0.2 \mu\text{m}$
220	LNE	$\sim 3 \cdot 10^4$ very stable	~ 18 very stable	1 mode $\sim 0.4 \mu\text{m}$
220	INRS	$\sim 2 \cdot 10^4$ very stable	~ 8 very stable	1 mode $\sim 0.3 \mu\text{m}$

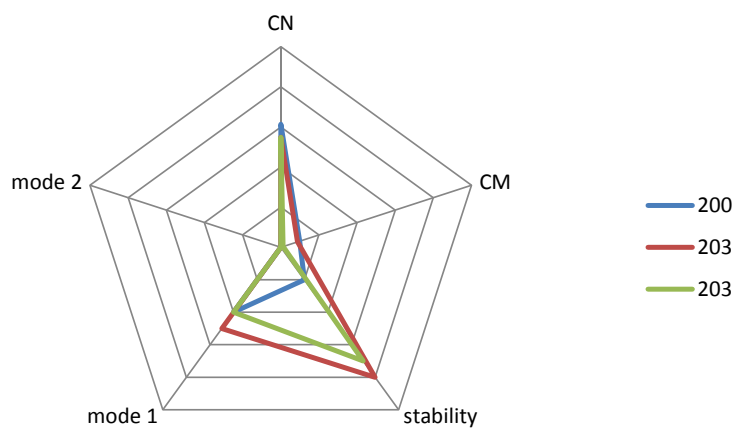
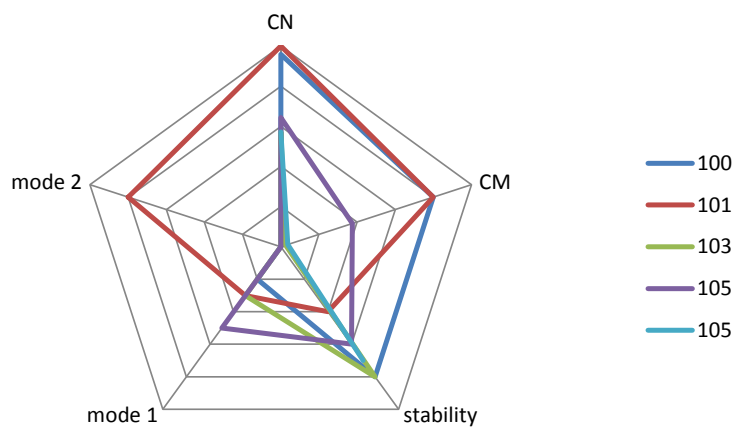
It should be noticed that these results were obtained using a specific generation device (RBG 1000, PALAS) associated with a sampling and dilution line; this makes the data not generic but valuable for this single case.

Again, the RBG was operated under constant conditions, which is among the reasons of concentration increasing with time due to the packing of the powder within the cylinder.

Figure 22 presents the different criteria gathered in Table 2 for the different groups of NM investigated (titanium dioxides, silicium dioxides, other NM). More precisely, the following parameters are reported according to a scale ranging from 0 to 5:

- the number concentration (CN): 0 = low concentration, 5 = high concentration ($> 10^7 \text{ cm}^{-3}$);
- the mass concentration (CM): 0 = low concentration, 5 = high concentration ($> 80 \text{ mg.m}^{-3}$);
- the stability over time: 0 = unstable, 5 = very stable;
- the modal diameter: 1 = 10 nm or below, 2 = 0.2 μm , 3 = 0.5 μm , 4 = 0.75 μm , 5 = above 1 μm .

It should be noted that two modal diameters are found for NM 101, which is why two possibilities for the mode are available in Figure 22.



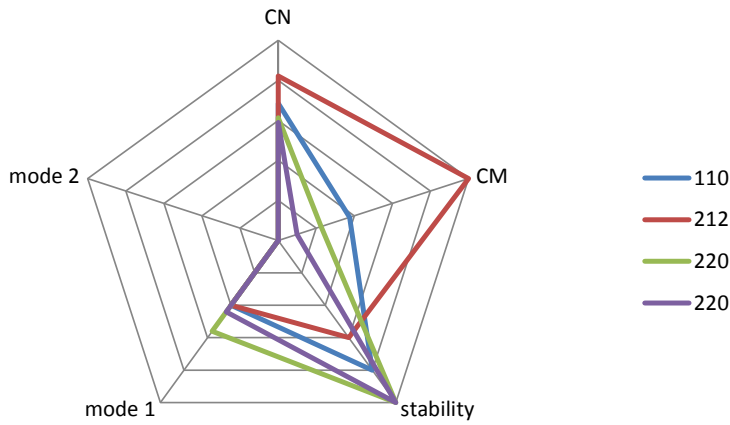


Figure 22. Schematic of the behavior of the different NM tested with the RBG 1000 generator.

To our point of view, the characteristics of powder-borne aerosols to be accounted for in toxicological studies rely in the combination of the parameters presented in Figure 22. Indeed, high number and mass concentrations are required, associated with the best stability over time. Information relative to the modal diameter of airborne particles is relevant when a given deposited amount of particles in the respiratory tract is sought.

4.2.3 Direct-synthesis method – Spark discharge generator (SDG) and evaporation/condensation in a high temperature (HT) furnace.

In this chapter is presented a thorough study of generation and thorough characterization of gas-borne nanoparticles (by spark discharge and evaporation/condensation), to be used for toxicity studies. This work has been performed by LTH (partner 37).

Metal nano particles were generated from different bulk materials: Pd, Ag, Cu and Au. The output characteristics of two spark discharge generators and a high temperature evaporation furnace were determined. The generated particles were measured using different on-line aerosol measurement devices and compared to TEM-analysis.

4.2.3.1 Description of the experimental set-up

A commercial spark discharge generator (SDGPalas, Palas model 1000), a high temperature evaporation furnace (HT), and an in-house spark discharge generator developed at Lund University (SDGC) were evaluated with regards to particle output and stability. Figure 23 shows the experimental set-up used for testing them (Svensson et al., 2015). The particle number size distribution was measured using a SMPS and the mass distribution using a DMA I series with an aerosol mass analyser (APM). The mass size distribution of an aerosol of aggregates can be determined using the DMA-APM in combination with a condensation (CPC) particle counter. The DMA, used at different voltages, upstream the APM was used to select monodisperse particles of varying sizes to the APM and the CPC downstream to count the number concentration. When both the mobility diameter and particle mass is known, the effective density, ρ_{eff} , and dynamic shape factor, χ , can be calculated.

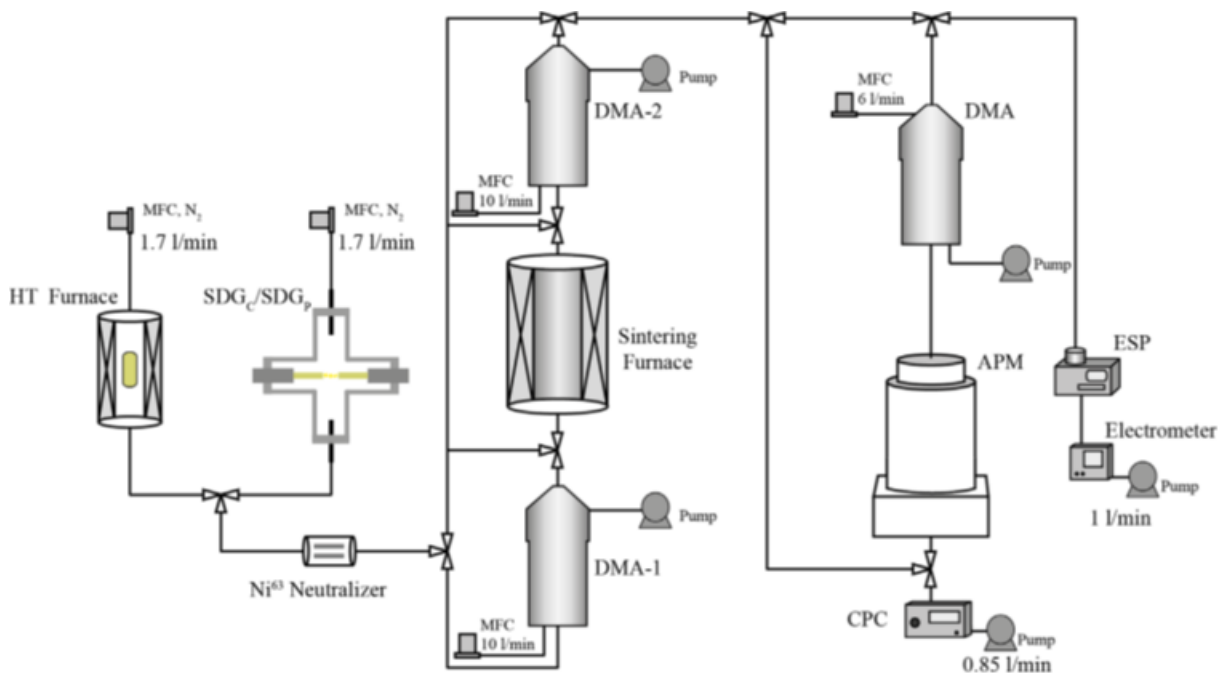


Figure 23. The set-up for the different generators followed by option for sintering using a furnace and on-line measurement of particle number and mass distribution as well as sampling on substrate for pre-sequent TEM-analysis.

4.2.3.2 Results obtained for Au, Cu, Pd and Ag aerosols

All generators were stable and Figure 24 shows an example of the SDGC generator output over 1 hour operating for Cu, Pd and Ag aerosols. Results of measured number size distributions for the different gold aerosols are shown in Table 2 and TEM/images of gold aggregates using the different generators is shown in Figure 3.

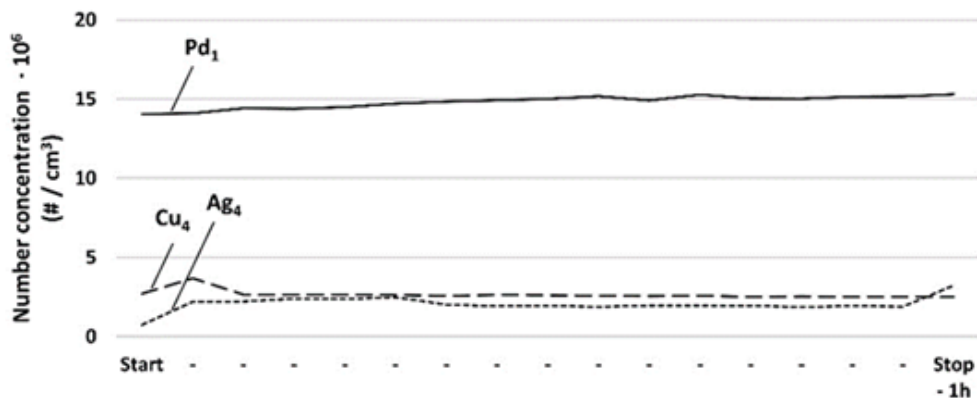


Figure 24. The output of the SDGC spark discharge generator with respect to total particle number concentration, reported from SMPS data. Aerosol particles of Pd, Cu and Ag aggregates were generated with a stable output during 1 hour periods.

Table 2. Characteristics of gold aggregates nano particles using different aerosol generators.

	CMD (nm)	GSTD	Number conc (#/cm ³)	Mass conc (mg/m ³)
HT 1575*	54	1.79	1.2 x 10 ⁸	34
HT 1625*	75	1.80	0.9 x 10 ⁸⁸	48
SDG _C **	78	1.92	0.9 x 10 ⁸	25
SDP _P 2.9***	28	1.64	1.9 x 10 ⁸	6.4
SDP _P 3.7***	28	1.65	2.0 x 10 ⁸	6.1

* Furnace generator at two different temperatures; 1575 and 1625 K, respectively.

** In-house spark discharge generator

*** Palas spark discharge generator running at two different flow rates; 2.9 and 3.7 lpm, respectively.

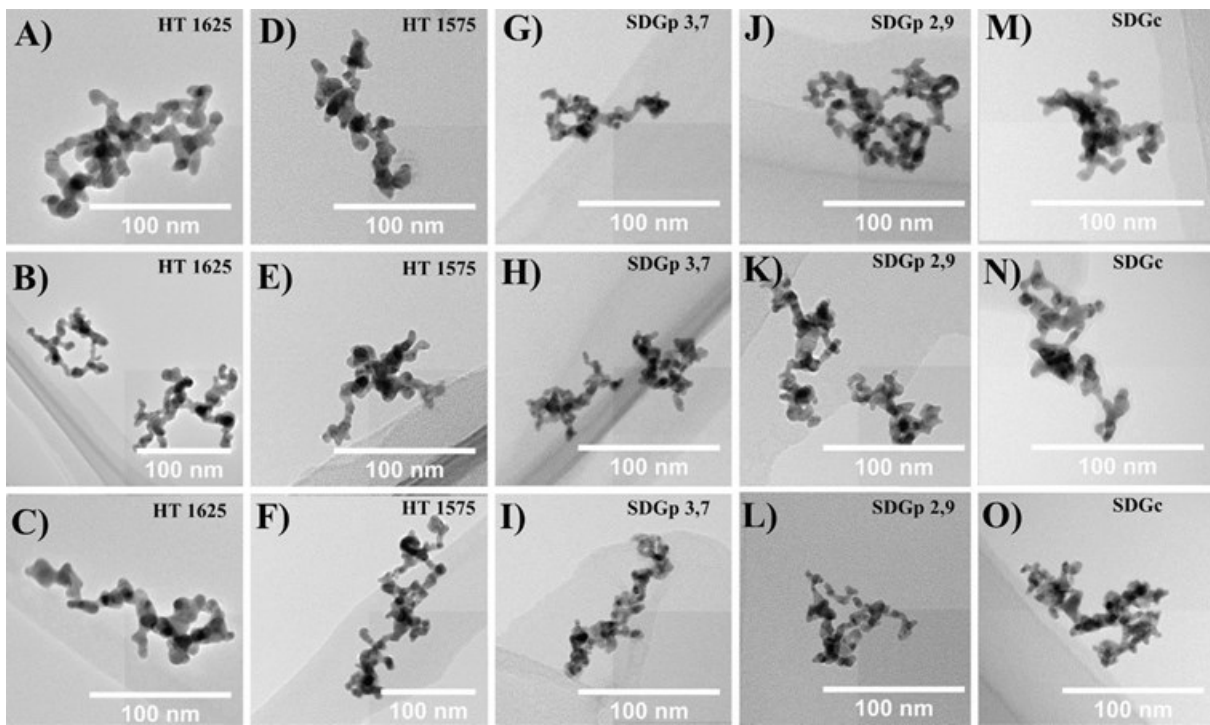


Figure 25: TEM-images of gold aggregates using the different generators (see Table 2).

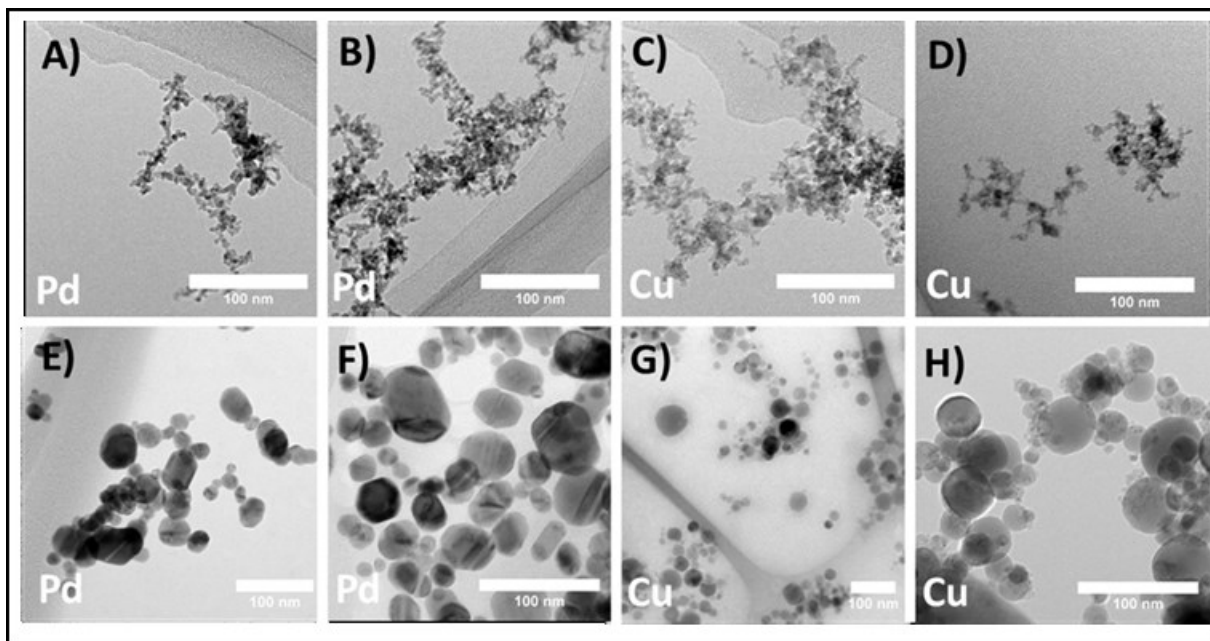


Figure 26: TEM-images of generated metal aggregates from bulk material from Pd and Cu using a spark discharge generator (in-house model). Picture A to D shows the aggregates and pictures E to H shows after sintering.

Using the particles characterizes measured by the APM (the effective density, ρ_{eff} , and dynamic shape factor, χ) and the TEM/analysis (primary particle diameter calculated as Sauters diameter) five different models (Table 3) was used to calculate the specific surface area, (SSA) and aggregate surface area.

Table 3: Overview of the input needed, empirical (DMA-APM, TEM, SMPS) and theoretical (DLCA), for specific surface area estimation using the five different approaches for calculation of aggregate surface area.

Approach	I	II	III	IV	V
DMA-APM	X	X			
TEM-analysis		X	X	X	
SMPS					X
DLCA-theory	X		X	X	

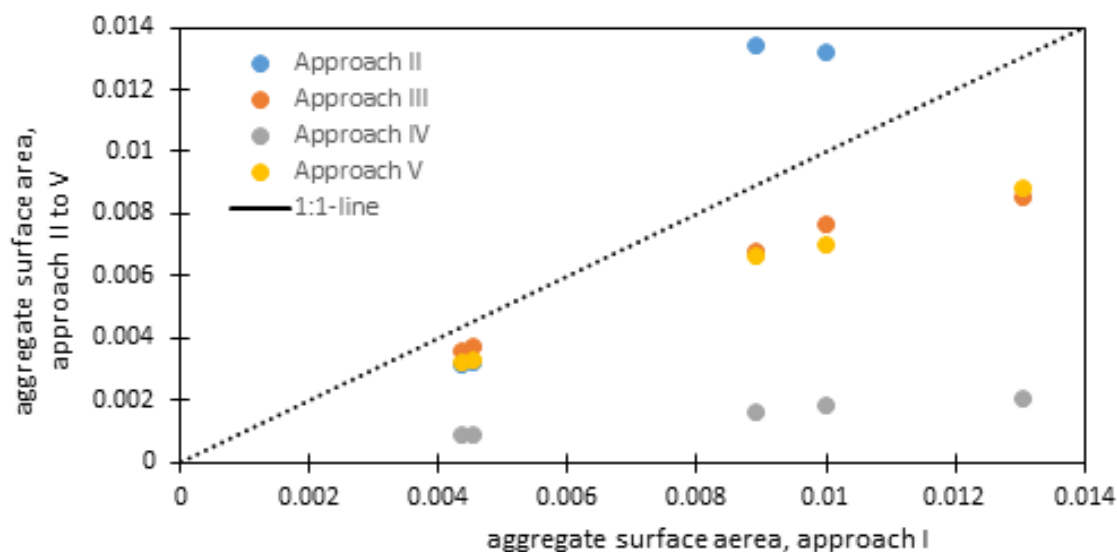


Figure 27. Comparison of estimated aggregate surface area: on-line measurement using the DMA-APM +DLCA-theory (approach I) versus approaches including TEM-analysis, approach II to V.

The model DMA-APM +DLCA-theory shows good agreement with approach III and V.

4.2.3.3 Exposure estimation (particle number, surface area, and mass size distribution)

The exposure with respect to particle number concentration and number size distribution was determined directly from the SMPS – for aggregates or spherical particles.

In addition to particle number concentration also mass and mass size distributions were determined by combining the SMPS measuring particle number size distribution and the DMA-APM estimating the mass distribution for each mobility size fraction. Firstly, the number size distribution is transformed into a mass size distribution:

$$dm/d\log D_{P(d_{me})} = dN/d\log D_{P(d_{me})} \cdot m_{agg(d_{me})}$$

The aggregate mass, m_{agg} , is estimated from DMA-APM measurements for respective compound and generator. Using the mass size distribution, the total mass concentration, c_m , is calculated integrating over $dm/d\log D_{P(d_{me})}$. The total mass exposure was also determined gravimetrically, showing a good agreement with the total concentration estimated by SMPS and DMA-APM.

The surface area distribution of the aerosols was obtained by multiplying above equation with the specific surface area, determined by the sauter diameter according to TEM described earlier:

$$dSA/d\log D_{P(d_{me})} = dN/d\log D_{P(d_{me})} \cdot m_{agg(d_{me})} \cdot SSA_{TEM}$$

The total surface area concentration is achieved integrating the function over size.

Both total mass and surface area can be estimated by more simple techniques such as gravimetric or chemical analysis, or by BET. However, since the lung deposition is strongly size dependent also mass size distributions as well as surface area distributions are needed in order to estimate the dose deposited in the respiratory tract. Thus, size resolved measurements of particles mass and surface area improves the dose estimates from lung deposition models such as the MPPD-model.

4.2.3.4 Comparison of different on-line aerosol instruments for airborne nanoparticles.

Three different types of nano particle sizing instruments (Fast Mobility Particle Sizer (FMPS), Electrical Low Pressure Impactor (ELPI) and Scanning Mobility Particle Sizer (SMPS)) and one only measuring number concentration Condensation Particle Counter (CPC) was compared in terms of size distributions and number concentration. The particle size range studied was 50 to 800 nm. The comparison was done using spherical oil droplets for 39 different sizes, with geometric mean diameter (GMD) ranging from 50 to 820 nm.

Test particles for the comparative studies were created by first aerosolizing a solution of NH₄NO₃ and water with a constant output atomizer using pressurized air of 1.5-3 bars depending on desired conditions. This aerosol was then dried using a diffusion dryer with silica gel to form salt particles with diameters of 40-50 nm. The dried salt particles were then introduced to the Condensation Aerosol Generator (SLG 250, Topas) where Di-Ethyl-Hexyl-Sebacat (DEHS) was condensed upon them to create spherical droplets. By varying the number of seed particles, oil temperature and flow rate through the saturator the oil droplet size could be varied from 50 nm up to 3 μm.

The results show that all three sizing-instruments agree well for particles sizes below 200nm, both in terms of determination of particle size and number concentration. Regarding particle sizing, the regression coefficient of SMPS versus ELPI was close to one ($R^2=0.98$) and no size-dependent shift in the comparison could be observed. The FMPS versus SMPS or ELPI the data correlates well ($R^2=0.94$) when particles sizes is below 200 nm, but for larger particle sizes it is clear that both FMPSs underestimate the particle sizes as compared to both SMPS and ELPI.

Comparison of measuring number concentration showed that there is a good correlation between SMPS and CPC (Ratio=1.03±0.04) and SMPS-ELPI (Ratio=0.98±0.14) in the whole particle size range studied. For the SMPS-FMPS number concentration comparison there is a similar scenario to that of particle size comparison. There is a good correlation up until 200nm (Ratio=0.99±0.12), but for larger particle sizes the FMPS number concentration starts to exceed the other instruments (SMPS and ELPI). The study concludes that particle distributions with a GMD above 200 nm cannot be measured reliably with the FMPS.

4.2.3.5 Conclusion

Metal nano particles were generated from different bulk materials: Pd, Ag, Cu and Au. The output characteristics of two spark discharge generators and a high temperature evaporation furnace were determined. The generated particles were measured using different on-line aerosol measurement devices and compared to TEM-analysis. The results show that all three of these generators produced a stable output of nanostructured metal agglomerate aerosol particles in the size range 30 to 300 nm, but at different mass concentrations ~5 to 50 mg/m³. Using an external furnace, the metal particles were sintered into nearly spherical particles. The generated particles were measured using different on-line aerosol instruments. More specifically, an aerosol particles mass spectrometer (APM) was coupled in series with a DMA and used to measure the true aerosol mass distribution for particles of a specific mobility diameter. This in combination with a SMPS scanning the particle number size distribution, the mass size distribution and surface area

distribution can be derived. Using the results the primary particle size was estimated and using five different models the aggregate surface was estimated. Comparison of the different models shows that on-line measurement using APM has good agreement with TEM-measurement. The developed method was applied on a mouse inhalations study. Finally, three different aerosol instruments for on-line measurement of particle number size distributions in the particle size range 10 to 700 nm was compared for spherical particles. The Fast Mobility Particle Sizer (FMPS), Electrical Low Pressure Impactor (ELPI) and Scanning Mobility Particle Sizer (SMPS) agree well for particles sizes in the range 10 to 200nm, both in terms of determination of particle size and number concentration, but for larger particle sizes it is clear that both FMPSs underestimate the particle sizes as compared to both SMPS and ELPI.

4.3 Characteristics of aerosols produced in a system for inhalation studies

4.3.1 NANOTIREX (*Nanomaterial Toxicology Inhalation system for Rodent Exposure, INRS*)

The experimental set up (Figure 28, Cosnier et al., 2016) consists of an aerosol generation system and inhalation towers for nose-only exposure (EMMS, Electro-Medical Measurement System, Bordon, UK).

Inhalation towers (Figure 29) are made from stainless steel and anodized aluminum to minimize electrostatic losses and reduce the possibility of contamination. Two types of towers were used: single level tower (9-port) for rats exposed to airborne nanomaterials and 3-level tower (3 x 9-port) for control rats; both have a by-pass flow (double plenum) designed to avoid mixing of inlet and exhaust flows (the one exhaled by the animals and the excess aerosol flow). Each exposure port has its own separated channel within the double plenum. The aerosol is directed to the exposure ports by means of a flow splitting cone from the central cylinder. Finally, rats held in restraining tubes attached to the towers are nose-only exposed to the aerosol. The total exposure capability is over 100 rats: 50 nanomaterials - exposed rats (exposed through 6 x 9-port tower) and 50 control rats (through 2 x 27-port tower). Aerosol generation was performed in a different room to inhalation exposure.

In line with OECD guidelines (OECD, 2009), the aerosol was conditioned at 22 ± 2 °C and relative humidity (RH) $55\pm 10\%$ by diluting it with air which had passed through a packed-tower humidifier. The diluted aerosol transited through stainless steel and antistatic perfluoroalkoxy tubing to reach the inhalation towers. In parallel, control rats were exposed to (particle-free) filtered air only (SMC IDG10-F03) (same air quality than that used for exposed rats) also conditioned at 22 ± 2 °C and RH $55\pm 10\%$. Airflows (5 L/min for exposure towers and 15 L/min for control towers) were pump-aspirated at the outlet of the towers to create a slight negative pressure (- 1.5 mbar). Both exposure towers and control towers were placed in containment boxes.

The integrated control of the exposure conditions (flow rates, temperature, RH, relative pressure, etc.) was managed and recorded using dedicated software. Aerosol monitoring and characterization were performed directly on the inhalation towers using a sampling probe fitting the conical portion of the restraining tubes

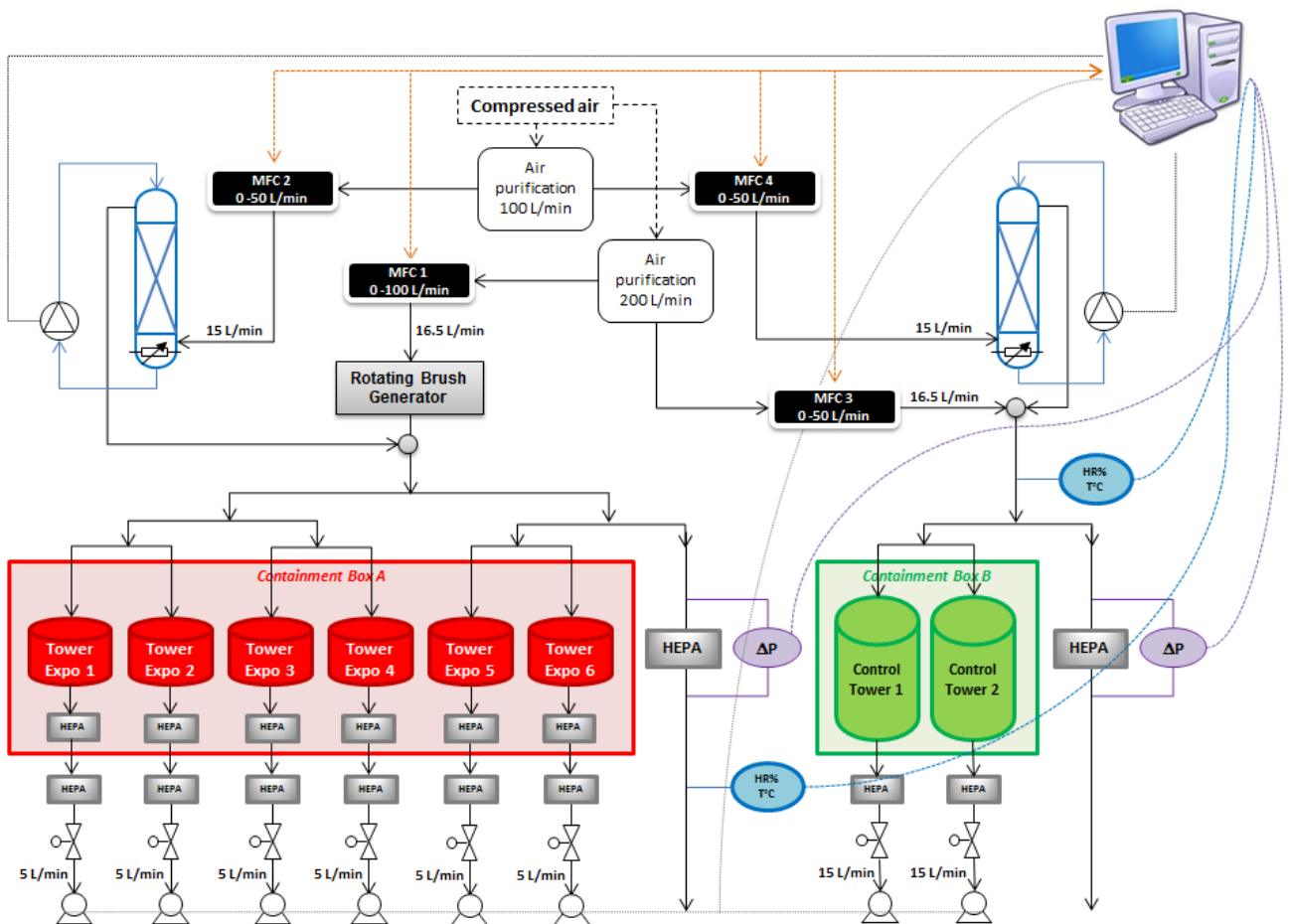


Figure 28. Schematic of the NanoTIREX facility.



Figure 29. Drawing of an inhalation tower equipped with 8 tubes and 1 sampling probe.

4.3.1.1 Case of titanium dioxide produced by the rotating brush generator (PALAS RBG1000)

In line with the strategy presented in Figure 3, the aerosols were characterized in detail by taking various measurements covering a wide range of particle sizes and properties. In particular, particle number size

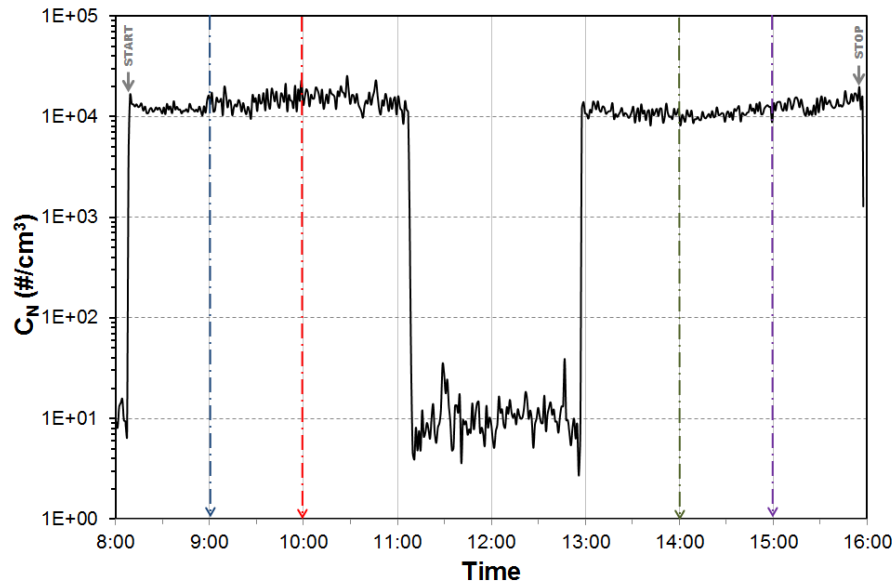
distribution was measured in the sub micrometer range (10 nm to 1000 nm) using a scanning mobility particle sizer (SMPS+C, Grimm, composed of a Vienna-type Differential Mobility Analyzer and a Condensation Particle Counter (CPC) 5.403; $Q_{\text{aerosol}} = 0.3 \text{ L}\cdot\text{min}^{-1}$, $Q_{\text{sheath}} = 3 \text{ L}\cdot\text{min}^{-1}$, $d_{50} = 4.5 \text{ nm}$). Data in the micrometer range (0.52 μm to 20 μm) were acquired with an aerodynamic particle sizer (TSI APS model 3321; $Q_{\text{aerosol}} = 5 \text{ L}\cdot\text{min}^{-1}$).

In addition, particle mass size distribution over a wide range of sizes, from 0.03 μm to 10 μm , was obtained with an electrical low pressure impactor (ELPI, Dekati, $Q_{\text{aerosol}} = 10 \text{ L}\cdot\text{min}^{-1}$). This mass size distribution was inverted by applying the procedure described above (Bau and Witschger 2013) and the collection efficiency curves described in Marjamäki et al. (2005).

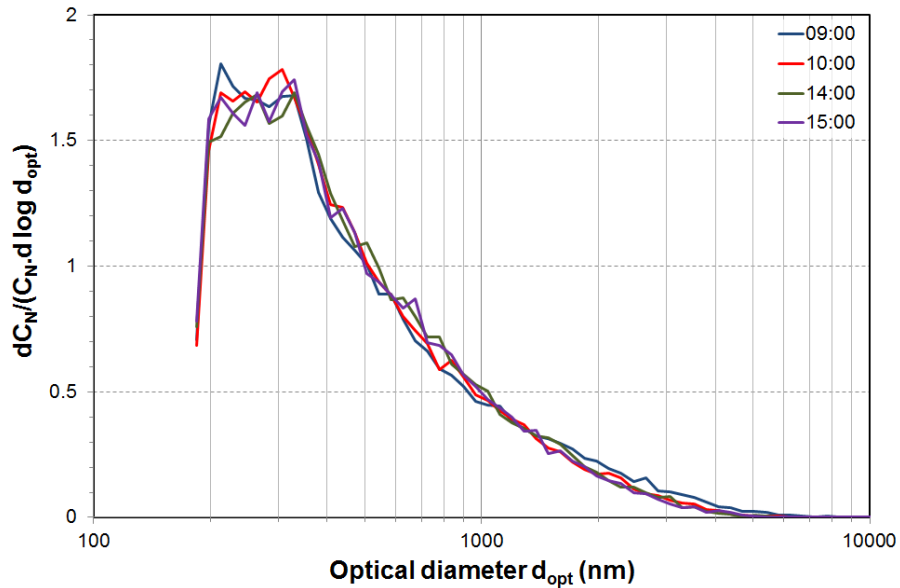
Finally, the electrical state-of-charge for particles was determined by combining airborne particle current and number size distributions measured by an ELPI, as detailed in Simon et al. (2015).

A typical profile of how the number concentration changes over time during exposure is presented in Figure 30. The daily variation coefficient of the number concentration never exceeded 15%. This profile was obtained from the raw data corrected for the dilution factor. Dilution was useful to avoid measurement problems, by maintaining particle coincidence within the OPC at less than 10%. By adjusting the feed rate of the RBG operated at constant air flow, an aerosol could be stably generated over six hours. In practice, the reservoir had to be filled twice a day with about 800 mg of dry powder, the powder bed was then pre-compacted before introducing it into the generator. Due to the high abrasiveness of TiO_2 P25 powder, the standard piston seal had to be replaced by a homemade Teflon seal. Number concentration profiles were measured with a CPC (TSI, model 3007, data not shown), with similar profiles obtained throughout the generation period and with each batch of powder. The average number concentration during the six 20-day campaigns of exposure was 24,000 particles/cm³ (± 6400 Standard Deviation) (diameter > 10 nm).

As shown in Figure 30 (for a single day's exposure), stability of the relative number size distribution was also verified during the exposure periods for aerosols with a modal diameter around 300 nm.



a)



b)

Figure 30. Time profile of the number concentration (a) and corresponding number size distributions (b).

The number size distribution of airborne particles is presented in Figure 31, with error bars representing the 95% confidence interval. To merge the two data series, which involve two different concepts of particle equivalent diameter, the aerodynamic diameters measured by the APS were converted into mobility equivalent diameters. As shown in Figure 31, the number size distribution was monomodal, with particles ranging in diameter roughly from 40 nm to 3 μm . Experimental data were fitted by a lognormal model according to the Least Squares Method, the Count Median Mobility Diameter (CMMD) determined was 347 nm, with a Geometric Standard Deviation (GSD) of 2.29. Expressed in terms of aerodynamic diameters, this resulted in a Count Median Aerodynamic Diameter (CMAD) of 269 nm, with a GSD of 2.22.

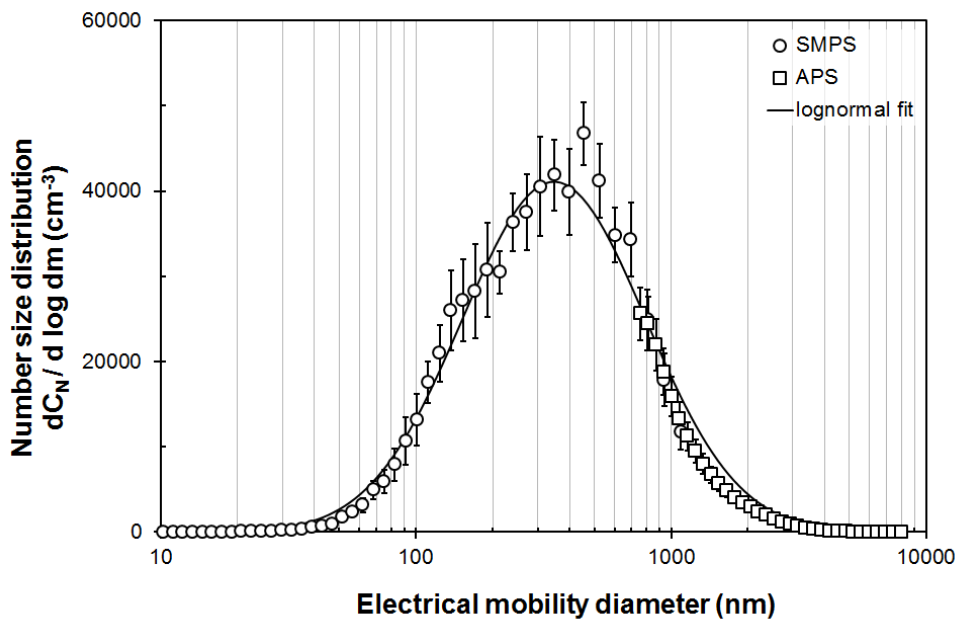


Figure 31. Number size distribution of airborne particles produced from TiO₂ P25 (NM 105).

The “routine” use of the cascade impactor allowed robust characterization of the airborne particles mass size distribution (Figure 32). The data presented in this figure represent the mean from 24 measurements. Figure 32 also presents ELPI data, calculated from the current size distribution measured and converted into a mass distribution (Bau & Witschger, 2013).

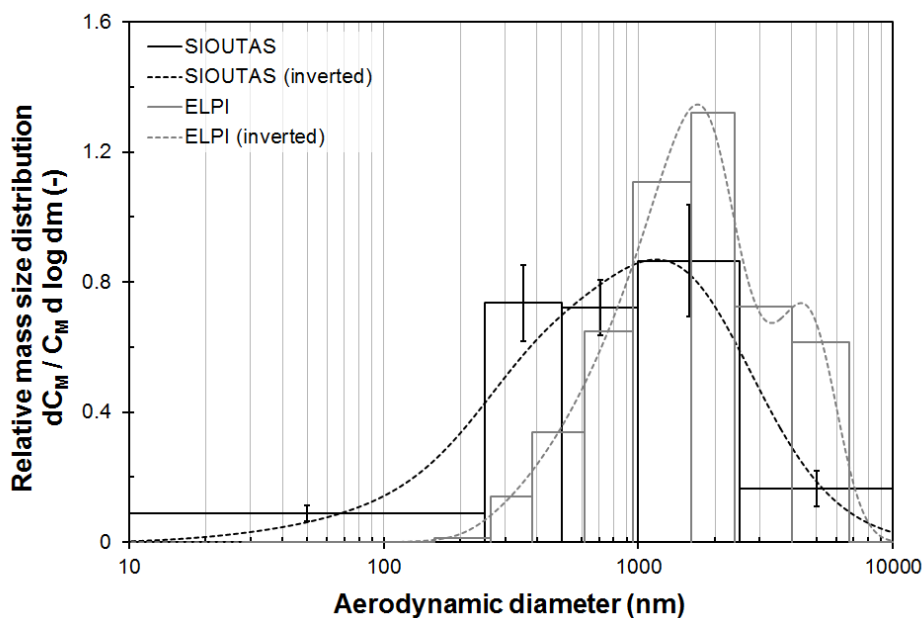


Figure 32. Mass size distribution of airborne particles produced from TiO₂ P25 (NM 105).

Finally, measurements were performed with the ELPI with and without a charger and ion trap to determine the average number of electrical charges carried by particles (Simon et al., 2015). Because charging mechanisms are related to the electrical properties of particles, the data were expressed as an electrical mobility equivalent diameter (Figure 33). The results indicate a negative state-of-charge; the number of

elementary charges varies from -4.3 [e] for 400-nm particles to -390 [e] for 6600-nm particles. In addition, the curve describing $p(d_m)$ is well fitted ($R^2 = 0.983$) by a power law, with an exponent of 1.57. This experimental curve fitting suggests that the surface area of airborne particles also affects charging mechanisms.

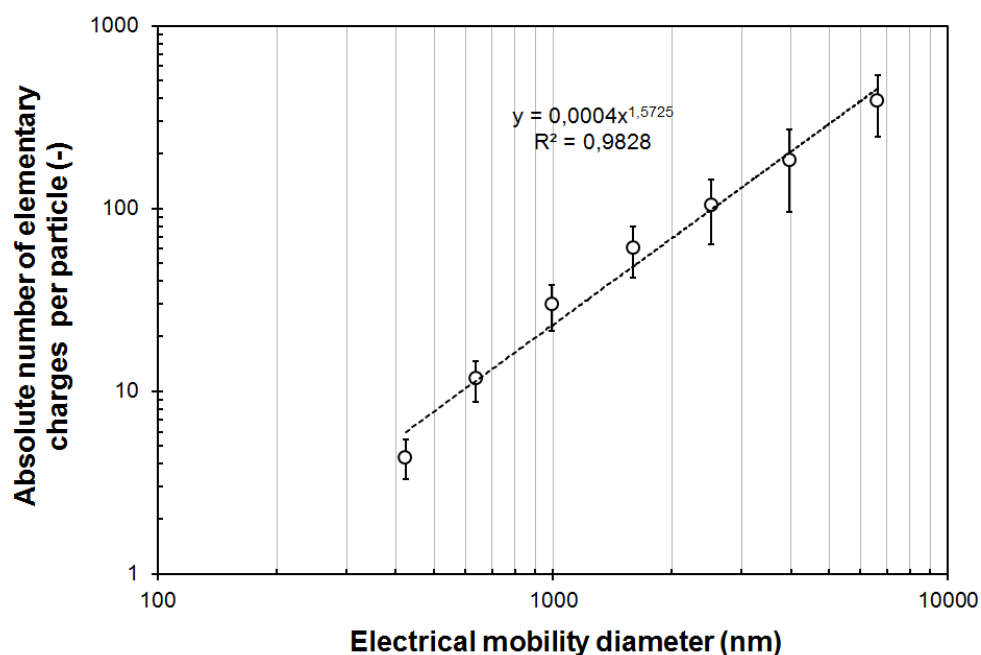


Figure 33. Evolution of the net number of electrical charges carried by airborne particles produced from TiO_2 P25 (NM 105).

4.3.1.2 Case of carbon nanotubes produced by a dry accoustic generator

In the experimental set up (Figure 28), only the aerosol generator was replaced specific system. This computer controlled multi-walled carbon nanotube aerosol generation system was developed by McKinney, et al. (2009) for the production of airborne carbon nanotubes. As illustrated in Figure 34, the major component of the generator is the large cylindrical acrylic chamber. Both ends of the cylinder are enclosed with flexible latex rubber diaphragms to form a drum-like structure. The diaphragms are held tightly in place with rubber o-rings. The cylinder is mounted vertically above a base containing a high compliance loudspeaker. The speaker faced upward, and without making physical contact was acoustically coupled to the bottom diaphragm of the acrylic cylinder. During operation, bulk samples of multi-walled carbon nanotubes (about 5 grams) are placed inside the cylinder onto the lower diaphragm. The speaker is driven with a computer and the signal used to excite the speaker was chosen to have frequencies above and below the resonant frequency of the acrylic cylinder and flexible diaphragm combination. HEPA filtered air enters the generator on the lower left hand side of the acrylic chamber, and exited the cylinder on the upper right hand side. In this configuration, the chamber acted as a vertical elutriator allowing only small airborne particles to escape the system. The larger particles consisting of agglomerated fibres and bundles tended to stay in the lower portion of the cylinder until there are dispersed.

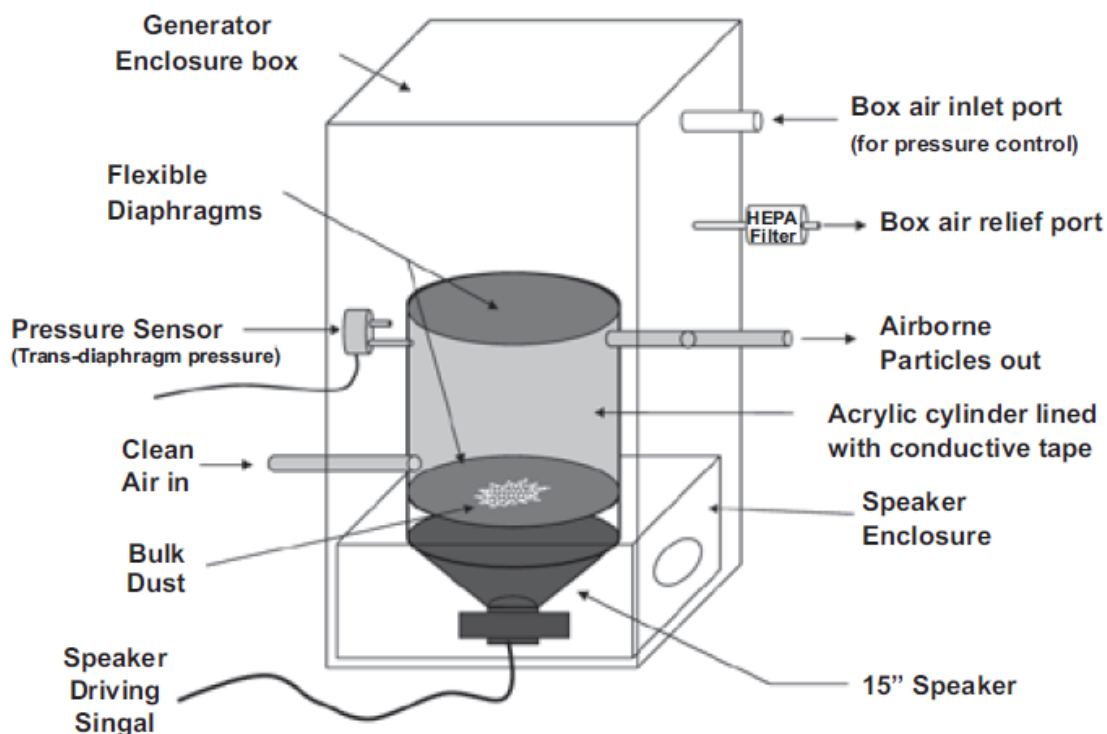


Figure 34. Illustration of the carbon nanotubes aerosol generator designed by McKinney et al. (2009).

For the rest, the same strategy as suggested in Figure 3 was employed for characterizing the test aerosol made of carbon nanotubes. The results shown below were recently presented at the European Aerosol Conference EAC 2016 (Cosnier et al., 2016).

➤ NM401

Figure 35 displays the number size distribution of airborne NM 401 produced by the dry acoustic generator obtained by three different instruments for in-depth characterization. It can be seen a good correlation between the different signals, with a modal diameter (aerodynamic) around 250 nm for SMPS data, and around 500 nm based on ELPI data.

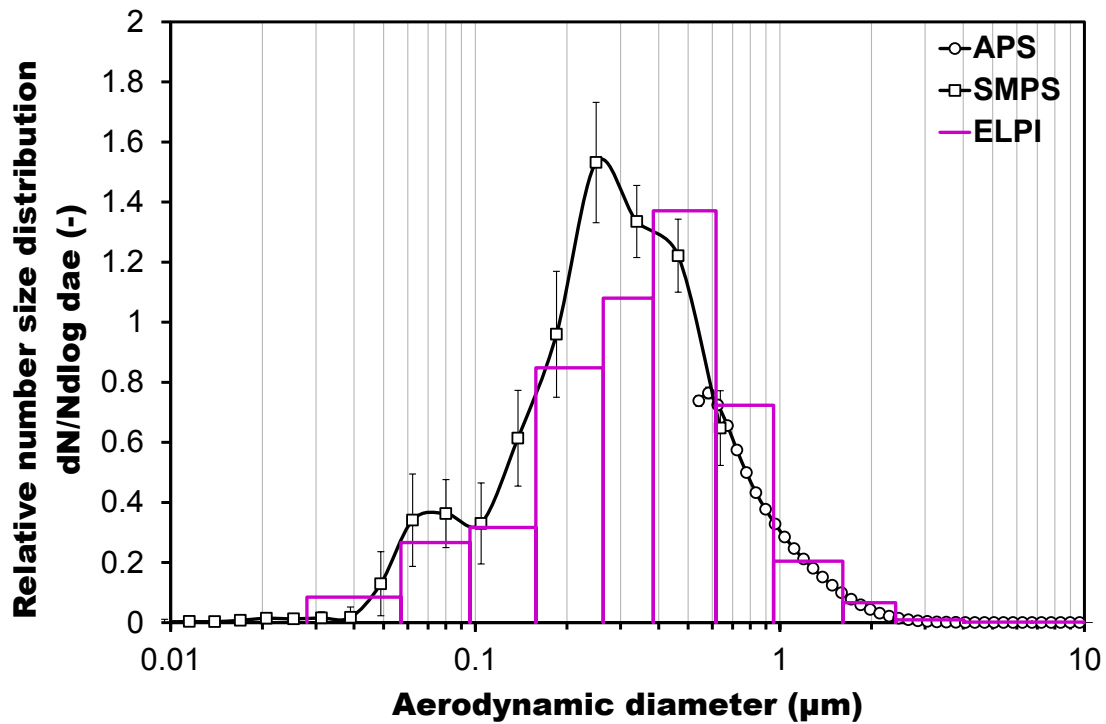


Figure 35. Number size distribution of NM 401.

The average mass size distribution is presented in Figure 36. The modal aerodynamic mass diameter is found to be around 0.8 µm, based on cascade impactor (SIOUTAS) data.

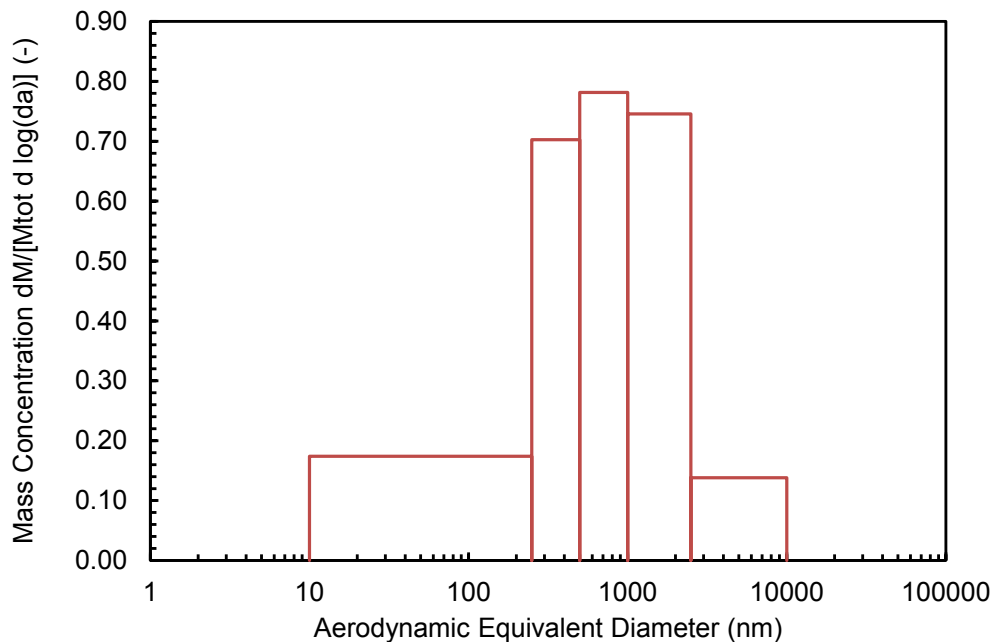


Figure 36. Mass size distribution of NM 401.

The characterization of the aerosols state of charge was also performed, as presented in Figure 37.

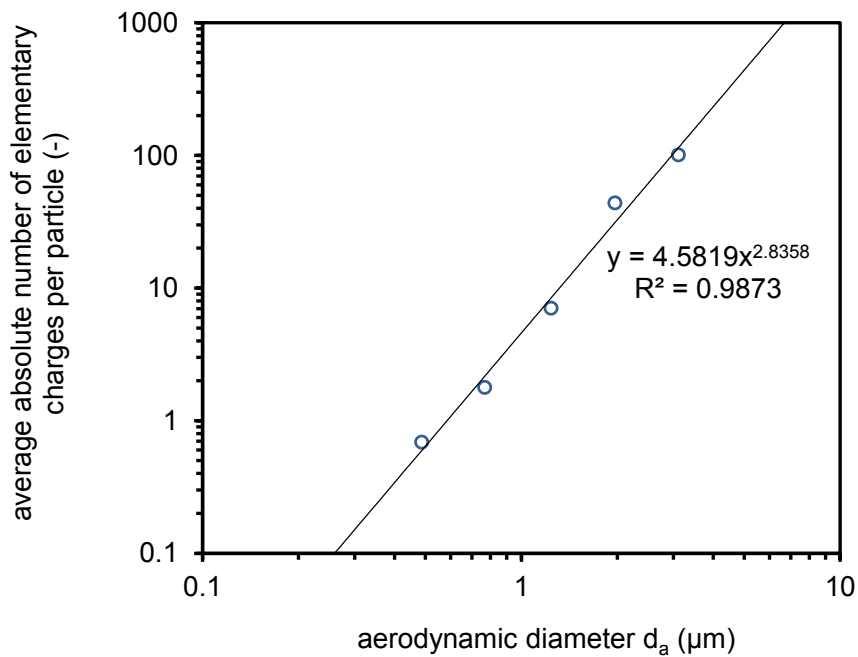


Figure 37. Evolution of the net number of electrical charges carried by airborne particles produced from NM 401.

➤ NM403

Figure 38 displays the number size distribution of airborne NM 403 produced by the dry acoustic generator obtained by two different instruments for in-depth characterization. It can be seen a good correlation between the different signals, with a modal diameter (aerodynamic) around 1.5-2 μm .

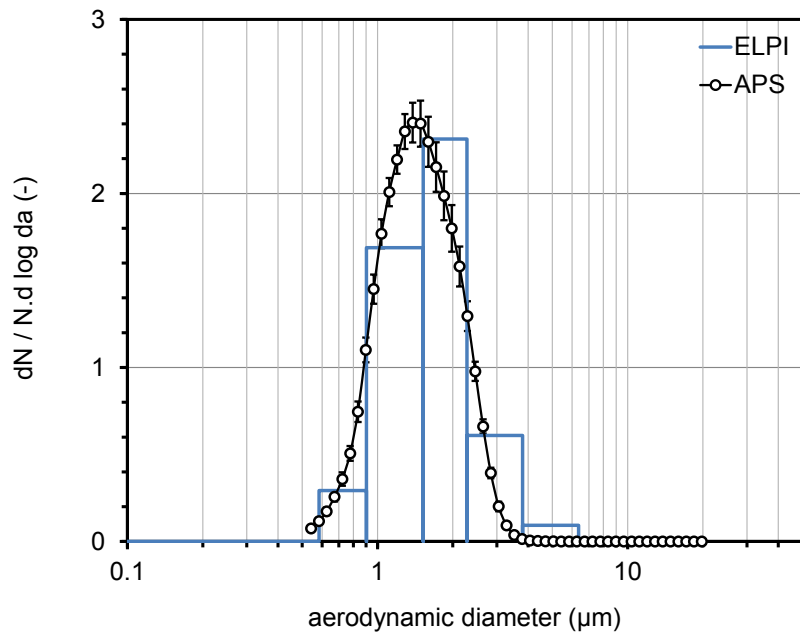


Figure 38. Number size distribution of NM 403.

The average mass size distribution is presented in Figure 39 . The modal aerodynamic mass diameter is found to be around 0.8 μm, based on cascade impactor (SIOUTAS) data.

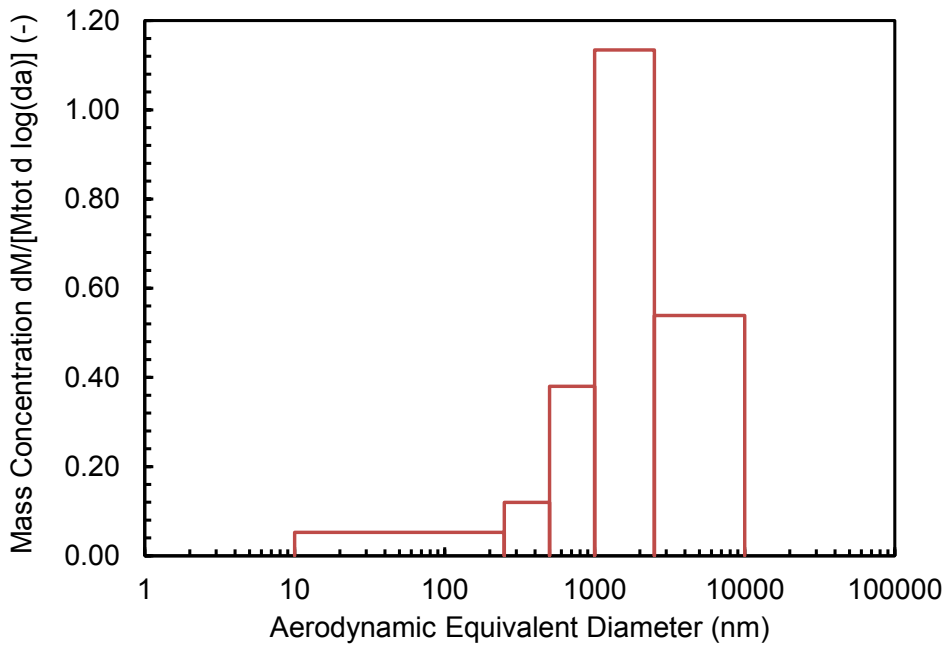


Figure 39. Mass size distribution of NM 403.

The characterization of the aerosols state of charge was also performed, as presented in Figure 40.

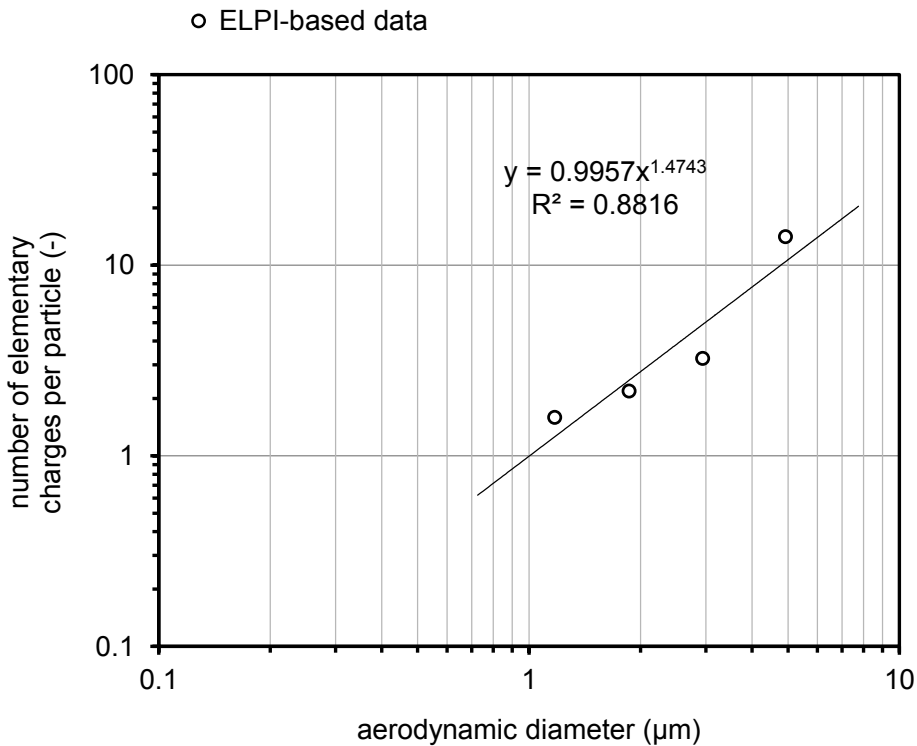


Figure 40. Evolution of the net number of electrical charges carried by airborne particles produced from NM 403.

4.3.2 NRCWE

4.3.2.1 Chemicals

The following metal oxide nanoparticles were included in the study: Al_2O_3 , CeO_2 , TiO_2 , and two types of ZnO (in the following referred to as ZnO_1 and ZnO_2). The Al_2O_3 , TiO_2 and ZnO_2 were synthesized by PlasmaChem (Berlin, Germany), CeO_2 and ZnO_1 were from Evonik Degussa, GmbH.

Selected data from the characterization of the particles is given in Table 4, which is based on Pérez-Campaña et al. (2012, 2013).

4.3.2.2 Generation of test atmospheres and aerosol characterization

All powders were aerosolized using a dry powder aerosol generator (Microdosing system, Fraunhofer ITEM, Hannover, Germany) as shown in Figure 41. The generator was operated at a pressure of 1.0 bar which generated airflow of 14.7 L/min. Concentrations in the exposure chamber ranged from 4-271 mg/m^3 . Particle size distributions of TiO_2 , Al_2O_3 , CeO_2 , ZnO_1 and ZnO_2 were characterized using an Electrical Low Pressure Impactor (ELPI+, Dekati Ltd., Finland) which measures the aerodynamic equivalent diameter in 14 channels ranging from 6 nm to 10 μm .

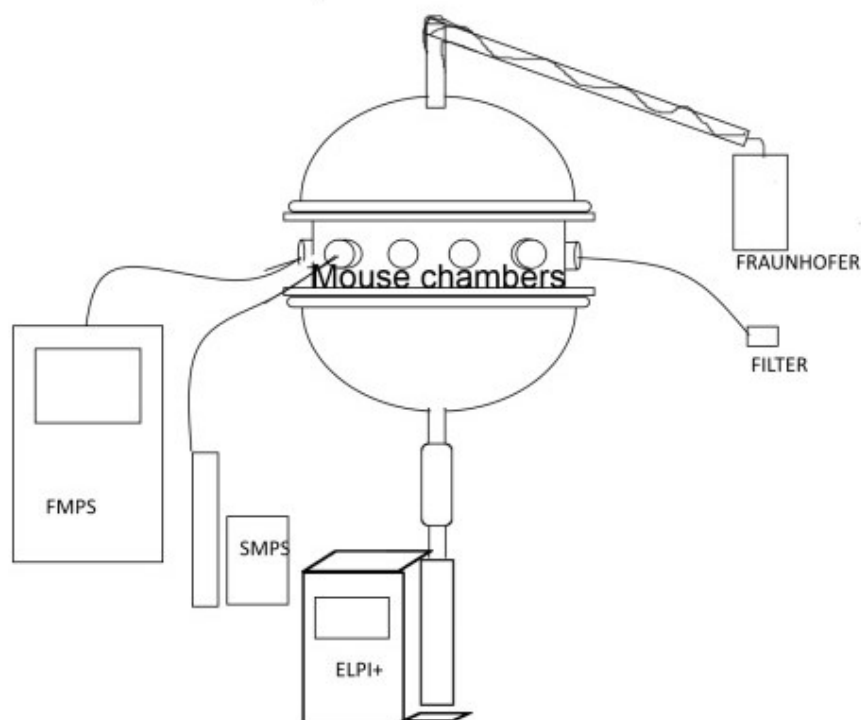


Figure 41. Present experimental set up for the instrument comparison using animal inhalation set up.

In addition, in order to compare different instrumentation to measure dispersed powders we used FMPS (Fast Mobility Particle Sizer, TSI, Model 3091) and SMPS. Airborne aerosol number concentration and number size distribution were measured on-line. FMPS will be used to measure number size distribution

from 5.6 nm to 560 nm (32 size bins) with one second resolution. SMPS was set to measure from 22.5 to 736.5 nm. SMPS and FMPS are both measuring mobility diameter, but different techniques. Advance with FMPS is high time resolution, however it has known problems (see e.g. Levin et al., 2015) and therefore SMPS is a good addition for the doing these kind of measurements. ELPI+ has a wide size and concentration range, which is always an advantage. The down side is the bad size resolution. In addition, since ELPI+ measures aerodynamic diameter it is easier to apply data directly to e.g. lung deposition models.

Table 4. Information of the studied powders.

Compound	Primary size (nm) Mean±SD	Characteristics	Specific surface area (m ² /g)	Density (g/cm ³)	Producer
Al ₂ O ₃	13.6±8.4	Polydisperse	76.3	4.0	PlasmaChem ¹ , Berlin
CeO ₂	13.0±12.1	Polydisperse	56.7	7.2	Evonik-Degussa
TiO ₂	1-10	Aggregated	173.1	4.2	PlasmaChem
ZnO_1	36.1±18.1	Polydisperse	21.9	5.6	Degussa-Quimidroga
ZnO_2	13.2±5.4	Monodisperse, aggregated	26.2	5.6	PlasmaChem

Data are from Pérez-Campaña et al. (2012, 2013)

Figures 42 to 46 present results from conducted measurements. Left panel in each Figure presents SMPS and FMPS+APS measurements, in these experiments Fraunhofer powder dispersion system was set in the level corresponding low level concentration in ELPI+ measurements.

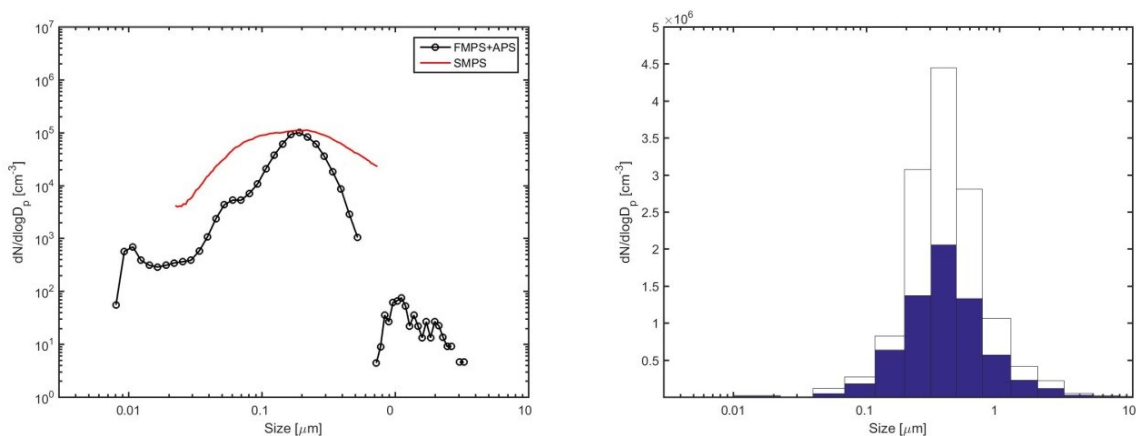


Figure 42. Number distribution at high and low concentrations for Al₂O₃ measured with ELPI+ and low concentration measured with SMPS, FMPS+APS.

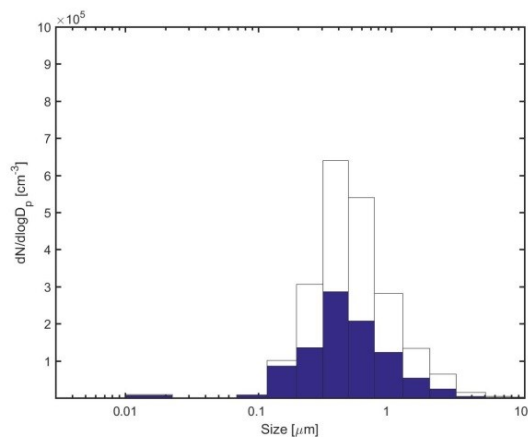
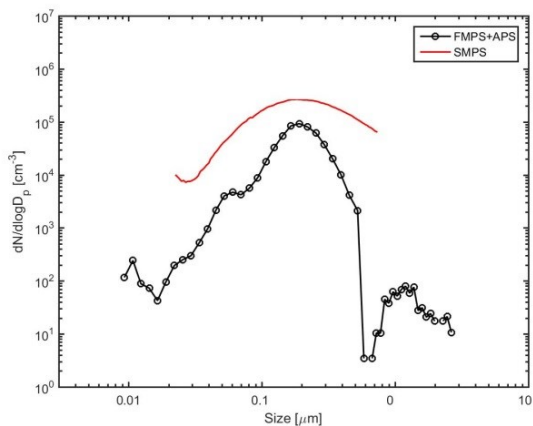


Figure 43. Number distribution at high and low concentrations for CeO₂ measured with ELPI+ and low concentration measured with SMPS, FMPS+APS.

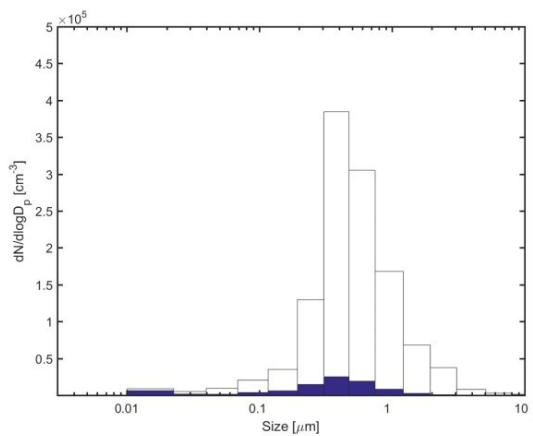
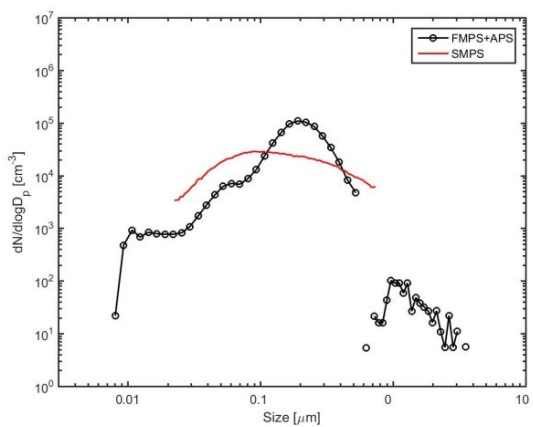


Figure 44. Number distribution at high and low concentrations for ZnO₂ measured with ELPI+ and low concentration measured with SMPS, FMPS+APS.

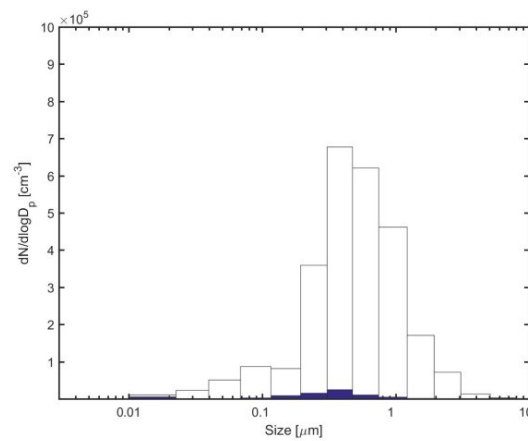
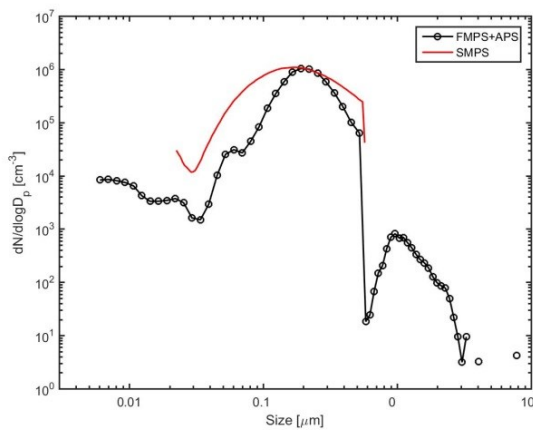


Figure 45. Number distribution at high and low concentrations for ZnO₂ measured with ELPI+ and low concentration measured with SMPS, FMPS+APS.

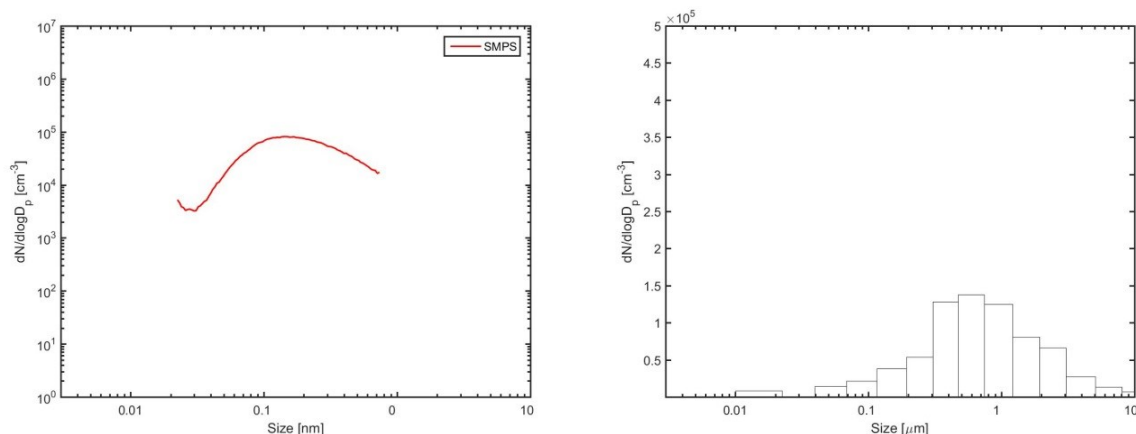


Figure 46. Number distribution at high and low concentrations for TiO₂ measured with ELPI+ and low concentration measured with SMPS, FMPS+APS.

4.4 Evaluation and conclusions

Inhalation is considered the gold standard for dosing the respiratory tract. The major advantage of inhalation exposure is that it mimics human pulmonary exposure by distributing the inhaled material throughout the whole respiratory tract in a physiological way over time.

The work was done along two axes:

- A literature review conducted in an objective to propose recommendations in terms of aerosol measurement strategy. The first objective was conducted mainly by LNE and INRS.
- Experimental work with the aim to characterize different test aerosols using different generation methods to be used for inhalation studies. The second objective was conducted by the four partners INRS, LNE, LTH and NRCWE.

The results clearly show several things:

- For dry-based method, where mechanical forces are added to dry nanomaterial powder, and the resulting separated particles are entrained in air, the test aerosols obtained cover the particle size range from about few tens of nanometers up to several micrometers. Test aerosols are mainly composed or aggregates and/or agglomerates that composed the nanomaterial powder. The conditions required for inhalation studies (stability, repeatability, level of concentrations) are sometimes difficult to obtain, but possible. Few generation devices are commercially available. Nevertheless, it is necessary to carry out preliminary tests in order to ascertain the performances of the chosen devices and their suitability for the inhalation facility. The dry-based method, apparently easy to implement, actually requires a good level of know-how and expertise in terms of generation and characterization.
- For direct-synthesis method, where airborne nanoparticles are synthesized in the gas phase and delivered to inhalation chambers as they remain suspended, the test aerosols obtained cover the particle size range from about few nanometers up to several hundred of nanometers. Higher concentrations in number can be obtained with this method. Also stability and repeatability is generally very good. Very few generation devices are commercially available. The development of such home-made generation system is a long-term task requiring a high level of expertise in terms of generation and aerosol characterization.

Altogether, the work carried out show that the generation and the characterization of the test aerosols for inhalation studies is an essential step but remains complex if one wishes to obtain robust results.

Beyond the recommendations proposed in Figure 3 (section 3), it is suggested that this phase should be carried out in collaboration with aerosol metrology specialists. It is this approach that has been implemented with success at INRS during the NanoREG project (see WP4 on carbon nanotubes and Cosnier et al. 2016) and NRCWE.

It is hoped that the recommendations proposed in this work can feed into the current work, into the current work, notably the revision of the OECD guidance document on inhalation toxicity testing.

5 Deviations from the work plan

This work was characterized by a strong experimental nature, the presence of several partners, and a not fairly clear initial objective. These elements have all contributed to the fact that work and the present deliverable were delayed. Nevertheless, several innovative methods were developed and experimental results obtained. This allows confirm the recommendations presented in Figure 3 for characterizing and monitoring test aerosols for inhalation toxicological studies.

6 References

- Bau S. and Witschger O. (2013). A modular tool for analyzing cascade impactors data to improve exposure assessment to airborne nanomaterials. *Journal of Physics: Conference Series* **429** 012002. doi: 10.1088/1742-6596/429/1/012002.
- Cosnier F., Bau S., Grossmann S., Nunge H., Brochard C., Viton S., Payet R., Witschger O. and Gaté L. (2016). Design and characterization on of an inhalation system suitable for rodent exposure to nanoaerosols of titanium dioxide. *Aerosol and Air Quality Research* **16**, 2989-3000.
- Cosnier, F., Bau, S., Grossmann, S., Viton, S., Nunge, H., Payet, R., Boivin, A., Witschger, O. and Gaté, L. (2016) Development and validation of an inhalation system suitable for rodent exposure to carbon nanotubes. *European Aerosol Conference, Tours, September 4-9*.
- Levin, M., A. Gudmundsson, J. H. Pagels, M. Fierz, K. Mølhave, J. Löndahl, K. A. Jensen, and I. K. Koponen (2015). Limitations in the Use of Unipolar Charging for Electrical Mobility Sizing Instruments: A Study of the Fast Mobility Particle Sizer. *Aerosol Science and Technology* **49** (8), 556-565.
- Marjamäki, M., M. Lemmetty, and J. Keskinen (2005). ELPI response and data reduction 1: Response functions. *Aerosol Science and Technology* **39**, 575-582.
- Morimoto Y., Horie M., Kobayashi N., Shinohara N. and Shimada M. (2012). Inhalation Toxicity Assessment of Carbon-Based Nanoparticles. *Accounts of Chemical Research*, 2012. **46**(3): 770-781.
- McKinney W., Chen B. and Frazer D. (2009). Computer controlled multi-walled carbon nanotube inhalation exposure system. *Inhal. Toxicol.*, **21**, 1053-61.
- Motzkus C., Gaie-Levrel F, Macé M, Vaslin-Reimann S (2014) Litterature review.
- OBERDÖRSTER G., CASTRANOVA V., ASGHARIAN B., & SAYRE P. - Inhalation Exposure to Carbon Nanotubes (CNT) and Carbon Nanofibers (CNF): Methodology and Dosimetry (2015) *Journal of Toxicology and Environmental Health, Part B*, **18**, 121-212.
- OECD (2009). *OECD Guideline for the testing of Chemicals*, 412.
- OECD (2012a) *Inhalation toxicity testing: expert meeting on potential revisions to OECD test guidelines and guidance document*. ENV/JM/MONO(2012)14.
- OECD (2012b) *Guidance on Sample Preparation and Dosimetry for the Safety Testing of Manufactured Nanomaterials*. ENV/JM/MONO(2012)40.

Perez-Campana, C., Gomez-Vallejo, V., Martin, A., San, S. E., Moya, S. E., Reese, T., Ziolo, R. F., & Llop, J. 2012, Tracing nanoparticles in vivo: a new general synthesis of positron emitting metal oxide nanoparticles by proton beam activation, *Analyst* **137**(21), 4902-4906.

Perez-Campana, C., Gomez-Vallejo, V., Puigivila, M., Martin, A., Calvo-Fernandez, T., Moya, S. E., Ziolo, R. F., Reese, T., & Llop, J. 2013, Biodistribution of different sized nanoparticles assessed by positron emission tomography: a general strategy for direct activation of metal oxide particles, *ACS Nano.*, **7**(4), 3498-3505.

Simon X., Bau S., Bémer D. and Duquenne P. (2015). Measurement of electrical charges carried by airborne bacteria laboratory-generated using a single-pass bubbling aerosolizer, *Particuology* **18**, 179-185.

Svensson, Christian LU ; Ludvigsson, Linus LU ; Meuller, Bengt LU ; Eggersdorfer, M. L.; Deppert, Knut LU ; Bohgard, Mats LU ; Pagels, Joakim LU ; Messing, Maria LU and Rissler, Jenny LU (2015). Characteristics of airborne gold aggregates generated by spark discharge and high temperature evaporation furnace: Mass-mobility relationship and surface area. *Journal of Aerosol Science* **87**. p.38-52